Enhanced multiplex immunolabeling in tissues

Technical Journal Club 26_03_2019

Francesca Catto

PhD student

Content

- Paper #1

Recombinant monoclonal antibodies for enhanced multiplex immunolabeling in brain

- Paper #2

Highly multiplexed immunofluorescence imaging of human tissues and tumors using t-CyCIF and conventional optical microscopes

Introduction_paper #1

- Monoclonal antibodies are commonly assumed to be monospecific, but anecdotal studies have reported genetic diversity in antibody heavy chain and light chain genes found within individual hybridomas.

- Hybridoma cell lines can die off, lose their antibody genes, or simply not grow when taken out of frozen storage — meaning that the source of a particular monoclonal antibody may be lost forever.

- Early fusion partners secrete an additional light chain which can complicate antibody gene cloning.

- Such antibodies may bind to more than one target, either because the antibody is actually a mixture of antibodies with multiple specificities, or simply because it is able to bind to several proteins.

- Having mAbs available in recombinant forms as recombinant mAbs (R-mAbs) offers numerous additional advantages.

Polyclonal vs Monoclonal antibodies production

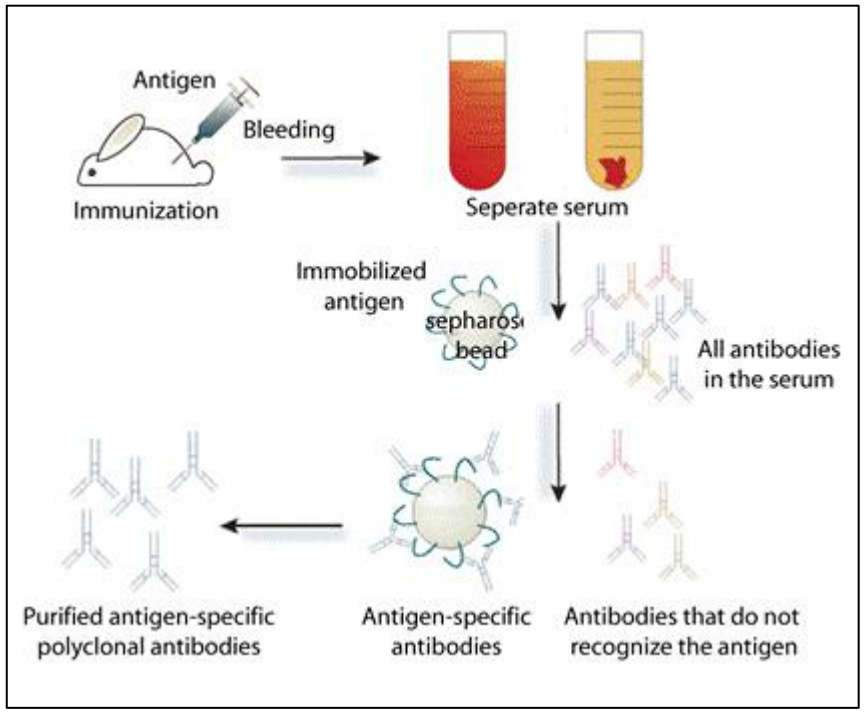

Polyclonal antibodies

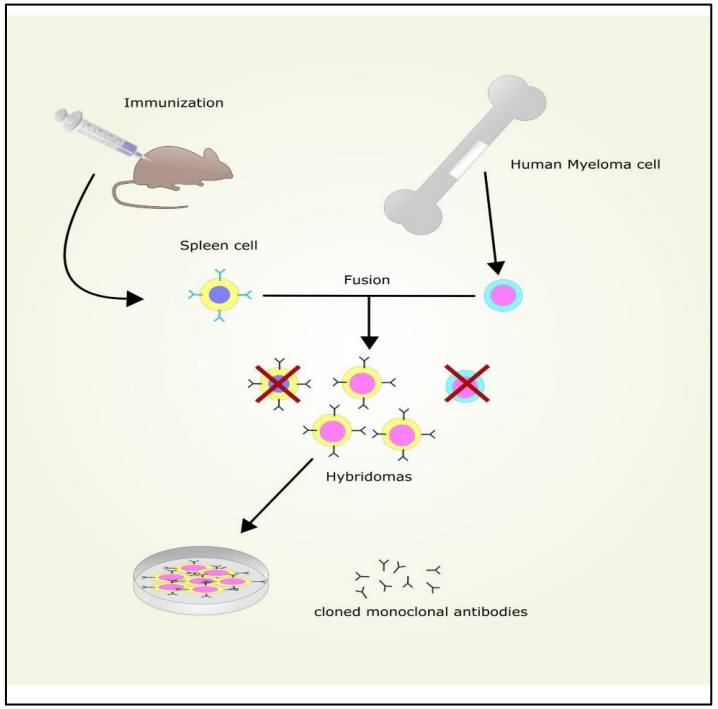

Monoclonal antibodies

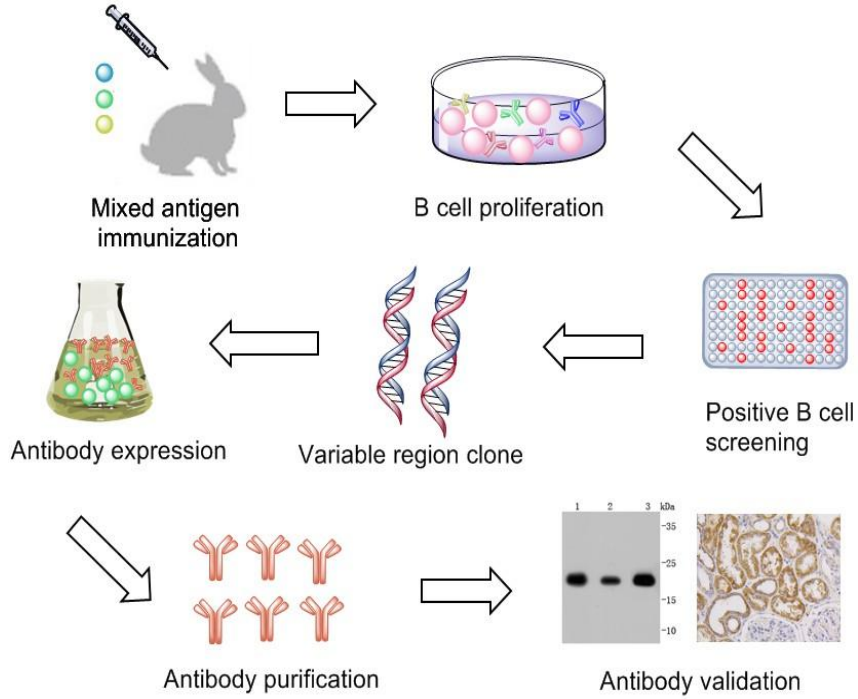

Recombinant monoclonal antibodies

Ways of producing RmAb

From hybridoma

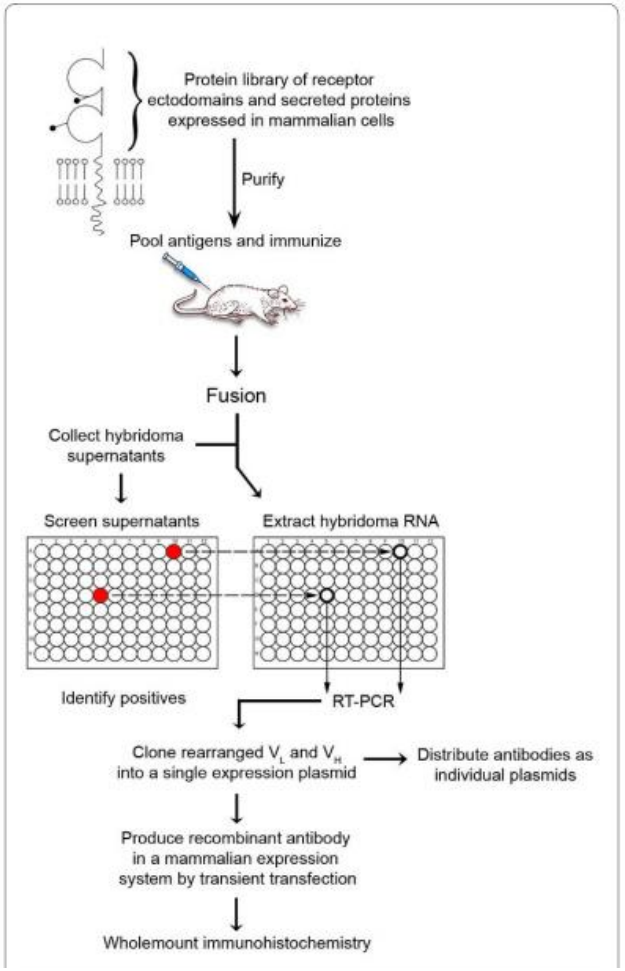

Crosnier et al., 2010).

From high complexity immune repertoire libraries

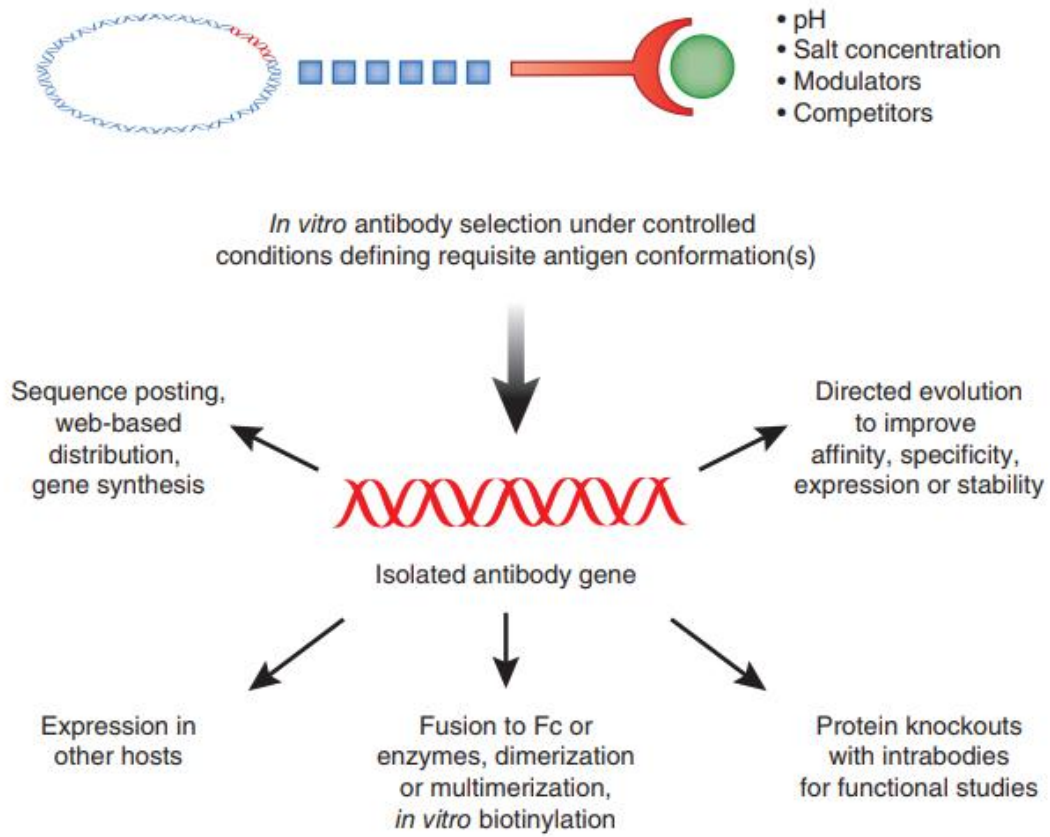

(Bradbury et al., 2011)

Advantages of recombinant expression

- Recombinant expression ensures production of a **single, molecularly defined** R-mAb.
- Recombinant expression can also yield **production levels hundreds or even thousands of times higher** than possible with endogenous expressions of mAbs from hybridoma cells (Fischer et al., 2015; Kunert and Reinhart,2016).
- The cloning of R-mAbs provides for **permanent, dependable and inexpensive archiving** of the R-mAb as plasmid DNA and nucleic acid sequences versus an archiving system relying on expensive cryopreservation of hybridoma cell lines in liquid nitrogen, and their subsequentrecovery as viable cell cultures.
- The conversion of existing mAbs to R-mAbs also allows for **more effective dissemination** of R-mAbs as plasmids, bacterial stocks or as DNA sequences.
- **Isotype conversion**.

Off-target binding effects

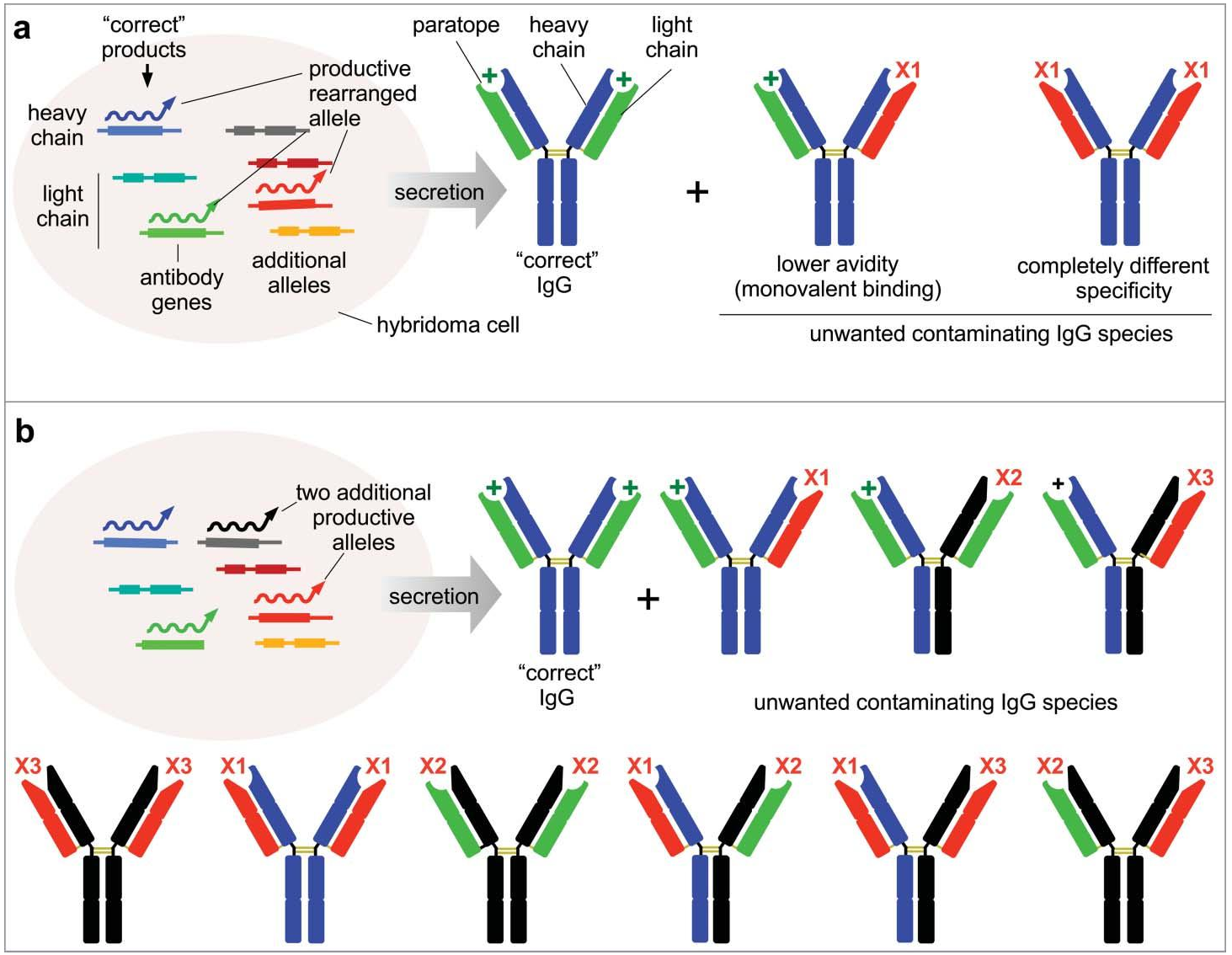

The possible reasons why hybridomas may express more than one HC or LC

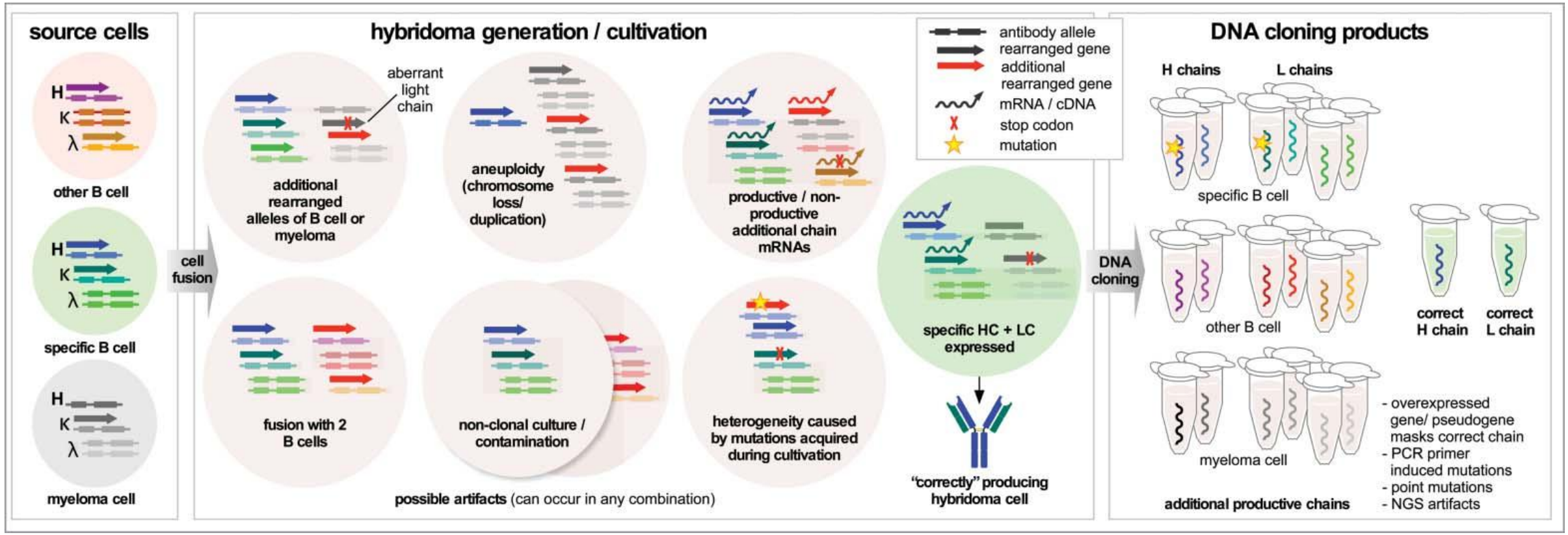

Multiplex labelling

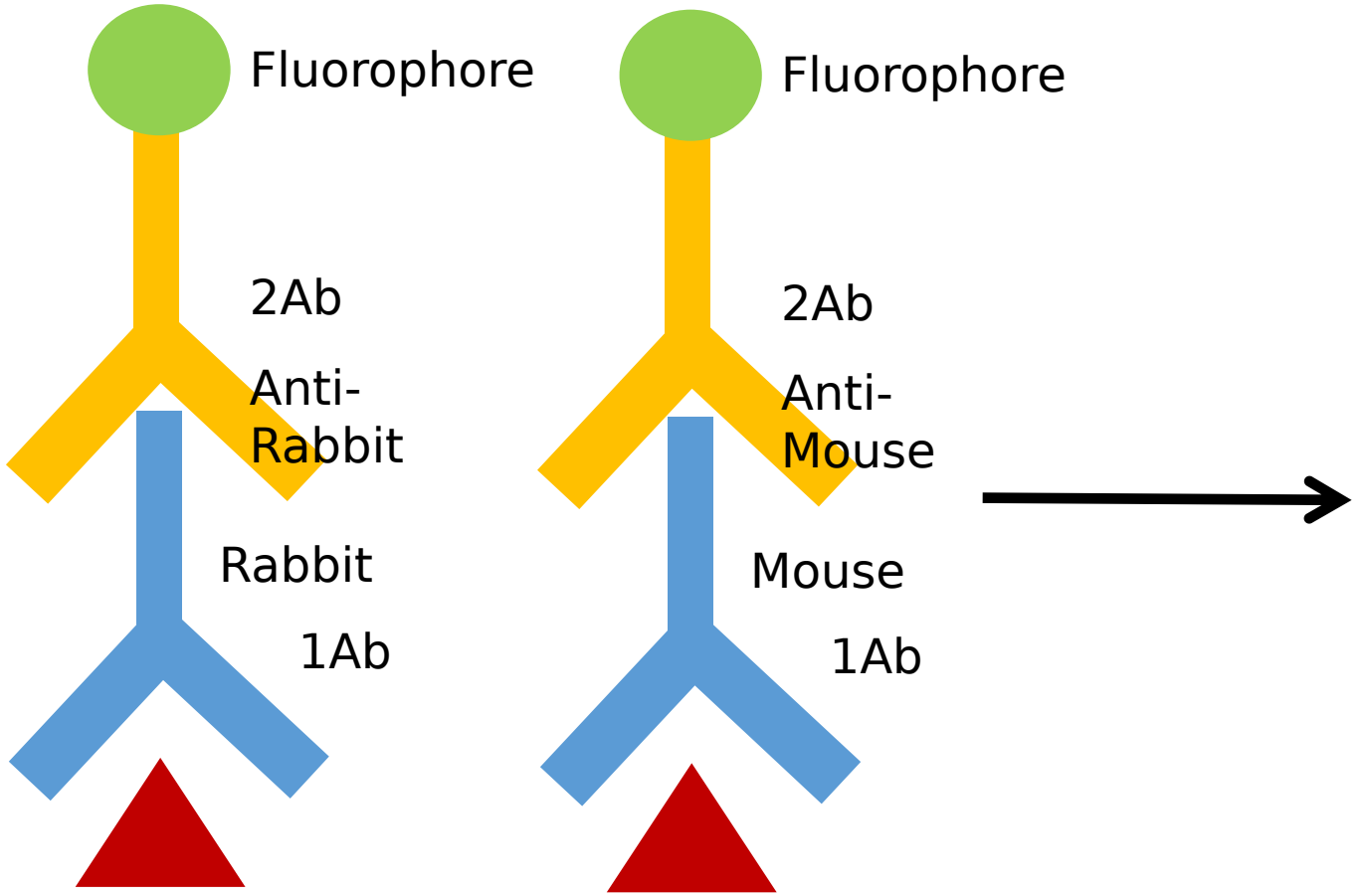

Each mouse mAb is a single immunoglobulin (Ig)
isotype - specifically of a single IgG subclass:
IgG1
IgG2a
IgG2b

Mouse mAb collections generally have an extremely high representation (» 70%) of IgG1 mAbs
--> limitation of the flexibility of multiplex labeling.

Conversion of mAbs to R-mAbs to make them different from their parents

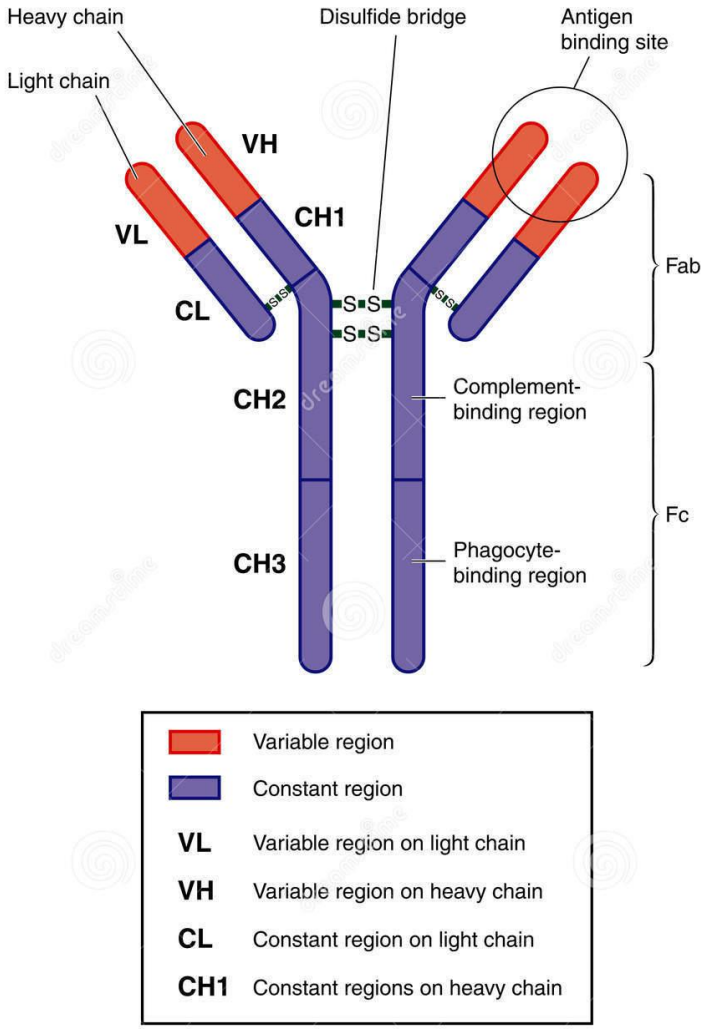

Switching the heavy chain constant region to impact subclass-specific secondary Ab binding specificity

Methods for Recombinant Monoclonal antibodies production from hybridoma cell lines

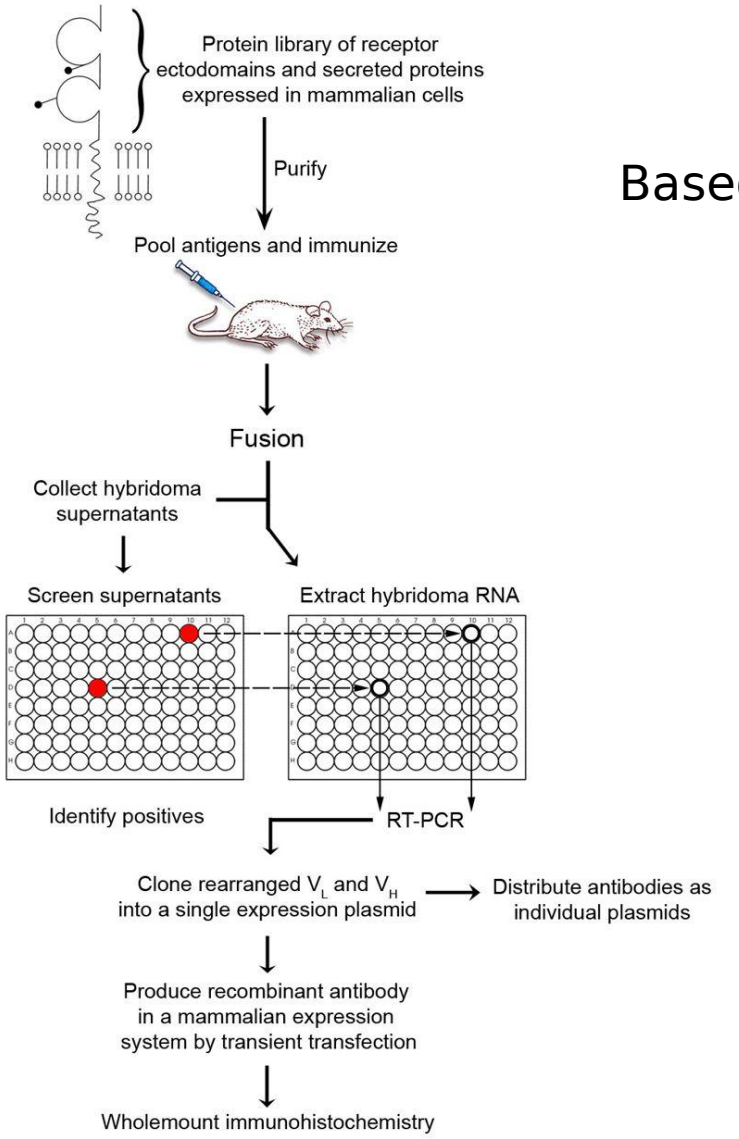

Based on standard animal immunization and hybridoma technology

- Heavy and Light chain loci were amplified from small numbers of selected hybridoma cells by RT-PCR.
- The amplified light and heavy chains were then joined into a contiguous PCR product and cloned into a mammalian expression plasmid so that large amounts of antibody could be quickly produced by transiently transfecting mammalian cells.
- Recombinant antibodies were then validated by staining fixed wholemount zebrafish embryos and the patterns checked for congruence with the known in situ expression profiles.

(Crosnier et al., 2010)

Paper #1

eLIFE elifesciences.org

TOOLS AND RESOURCES

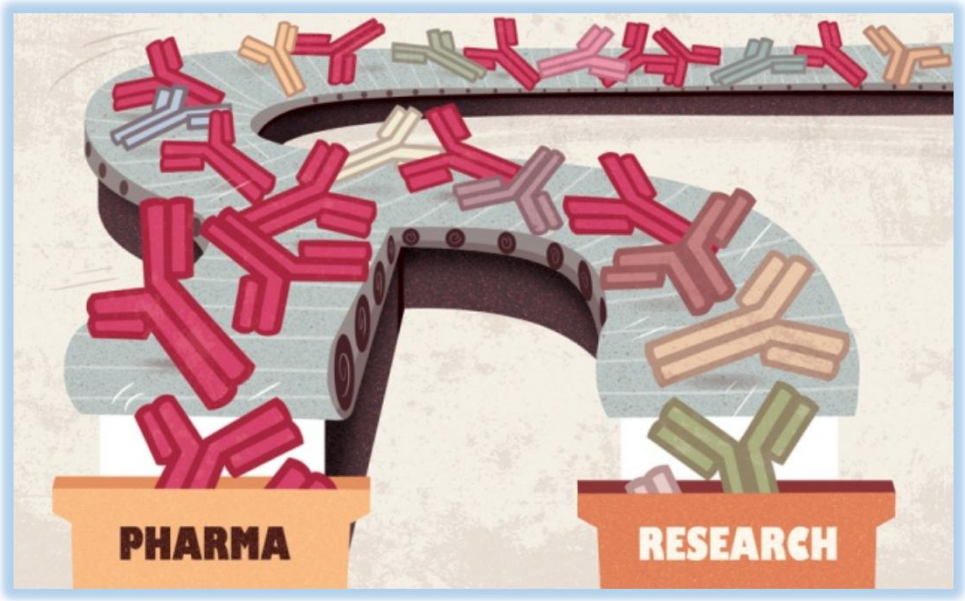

A toolbox of IgG subclass-switched recombinant monoclonal antibodies for enhanced multiplex immunolabeling of brain

Nicolas P Andrews[1], Justin X Boeckman[1], Colleen F Manning[1], Joe T Nguyen[2], Hannah Bechtold[2], Camelia Dumitras[1], Belvin Gong[1], Kimberly Nguyen[1], Deborah van der List[1], Karl D Murray[1], JoAnne Engebrecht[2], James S Trimmer[1,3]*

[1]Department of Neurobiology, Physiology and Behavior, University of California, Davis, United States; [2]Department of Molecular and Cellular Biology, University of California, Davis, United States; [3]Department of Physiology and Membrane Biology, University of California, Davis, United States

Published: 22nd January 2019

Overview

- Development of a coherent pipeline of protocols for effective cloning of intact R-mAbs from cryopreserved hybridoma cells and their subsequent validation compared to their parent mAbs.

- Development of a process to engineer these R-mAbs to IgG subclass-switched forms that provide additional utility for multiplex labeling employing mouse IgG subclass-specific secondary Abs.

- Achievement of a feasible and relatively inexpensive approach for any laboratory that uses standard molecular biology and mammalian cell culture techniques.

- Development of a reliable method to convert valuable cryopreserved hybridoma collections to the immortalized form of a DNA sequence archive, including hybridomas that are no longer viable in cell culture.

Effective cloning of immunoglobulin VH and VL regions from cryopreserved hybridomas and generation of R-mAbs

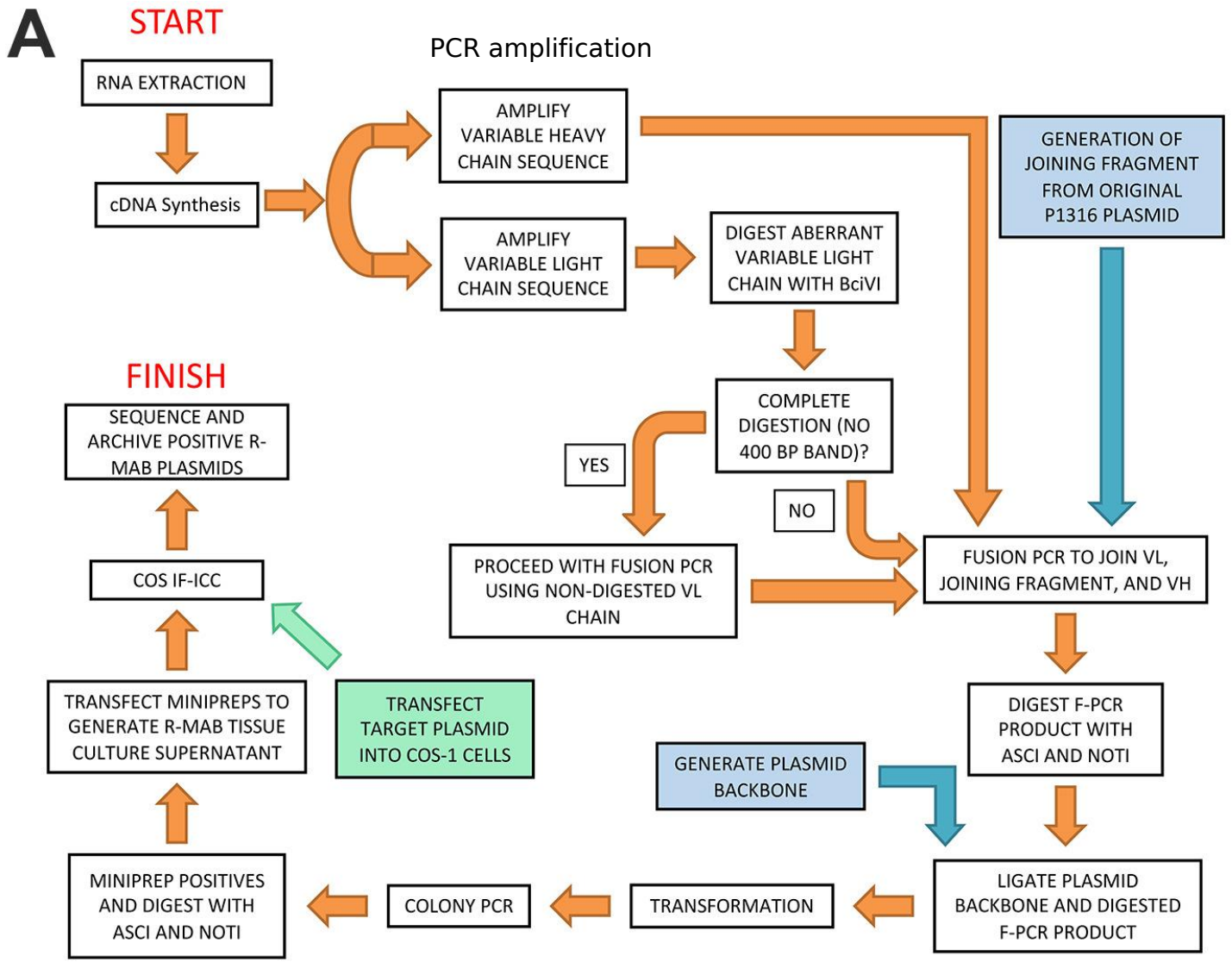

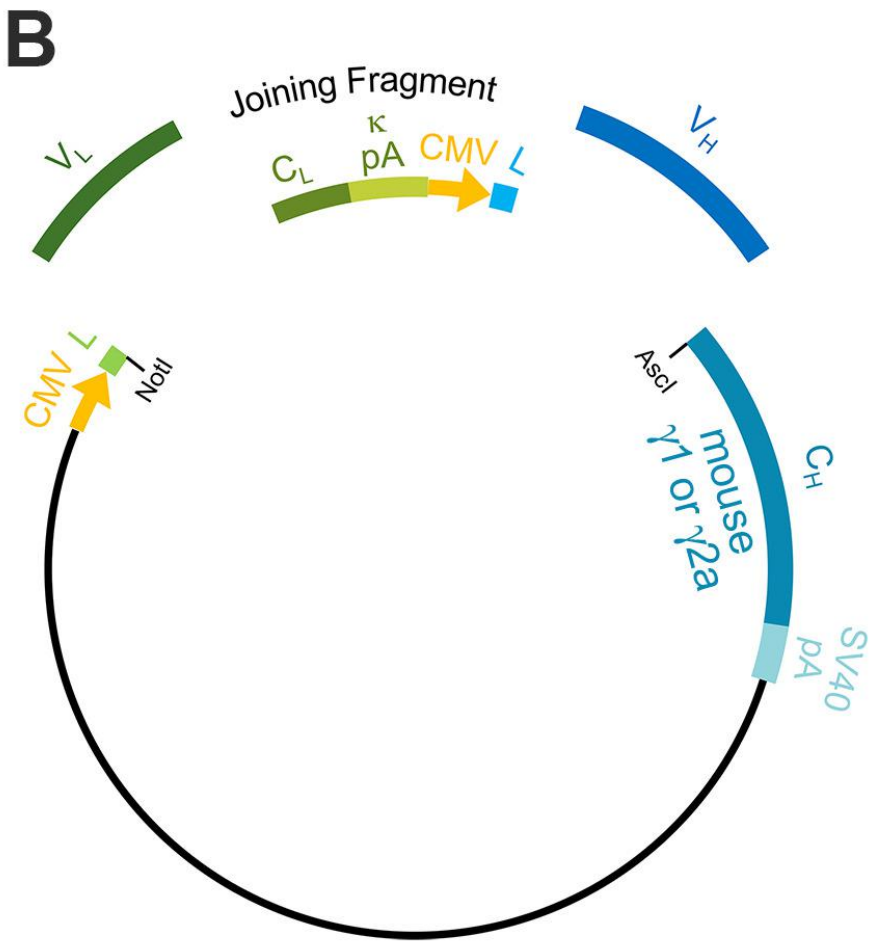

PCR products amplified from cDNA synthesized from RNA extracted hybridomas

N59/36 (anti-NR2B/GRIN2B) glutamate receptor
K39/25 (anti-Kv2.1/KCNB1) potassium channel

The expected size of mouse
IgG VL and VH domains is » 360 bp.

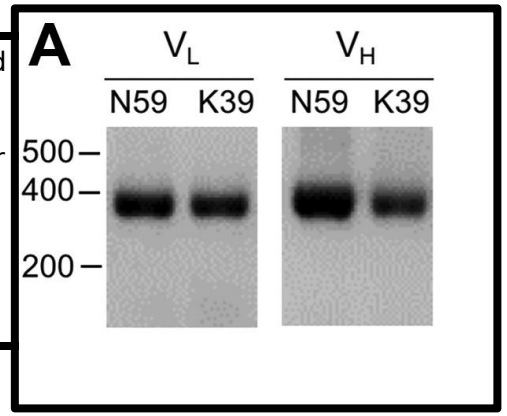

VH and VL PCR products + joining fragment amplified from the P1316 expression plasmid = 2.4 kbp amplicon

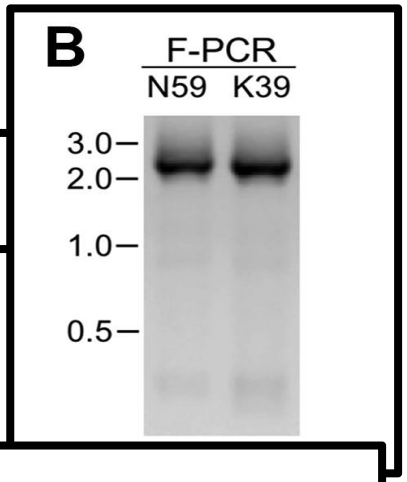

PCR:
Clones expressing the full-length IgG expression cassette

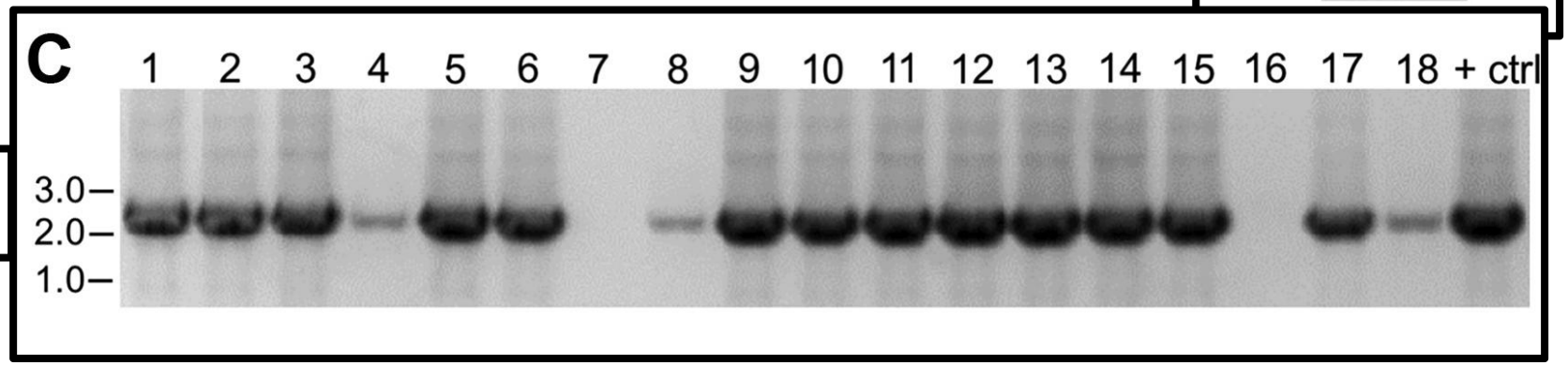

Restriction enzyme digestion of N59/36 plasmid DNA with NotI and AscI.

- plasmid backbone= 7 kbp
- intact insert comprising the V L and V H domains and the intervening joining fragment = 2.4 kbp.

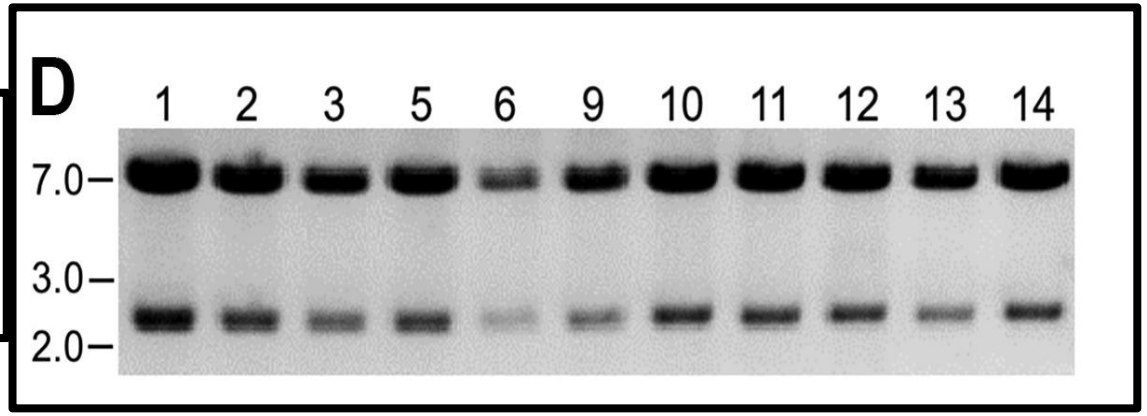

PCR products of VL domain cDNA synthesized from RNA extracted from
- mouse splenocytes
- fusion partner Sp2/0-Ag14
- various Sp/0-derived hybridomas
after digestion with the **BciVI** restriction enzyme to cleave the Sp2/0-Ag14-derived aberrant light chain product.

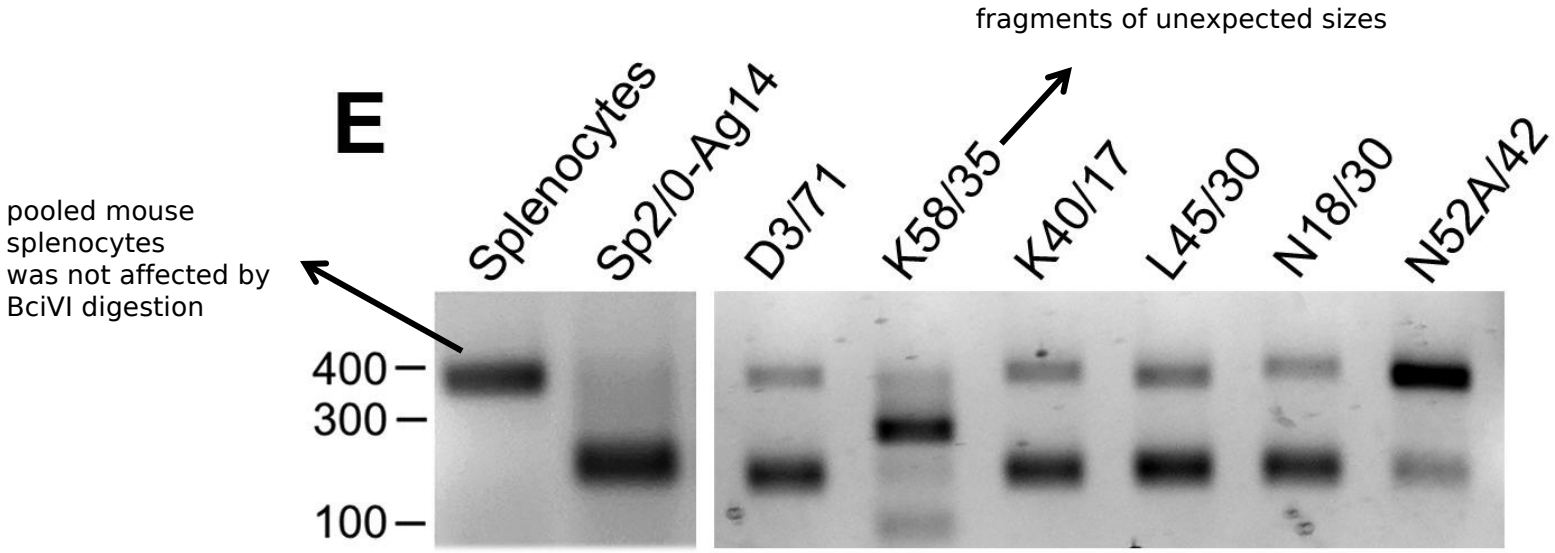

The intact VL domains are » 360 bp.
The digested aberrant light chains » 180 bp.

Testing RmAb by immunofluorescence in COS cells

Wells of COS cells tranfescted with full lenght target protein

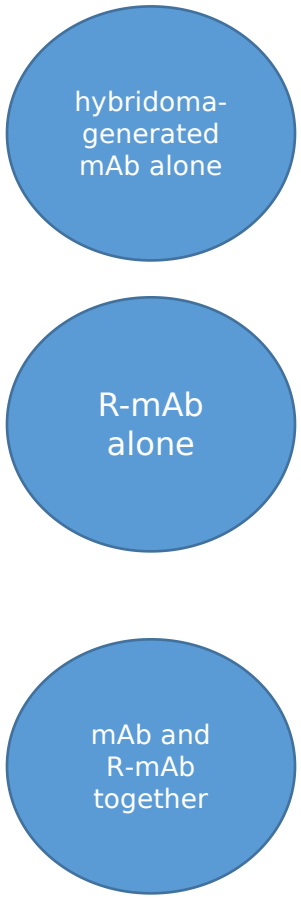

subclass-specific secondary Abs + Alexa Fluors.

What they want to demonstrate

- The target protein was expressed in a subset of the transiently transfected cells.
- The only detectable secondary Ab labeling was for the IgG subclass of the parent hybridoma-generated mAb.

- The R-mAb labeled a comparable number of cells.
- The only detectable secondary Ab labeling was for the IgG subclass of the subclass-switched R-mAb.

- mAb and R-mAb gave indistinguishable labeling patterns at both the cellular and subcellular.
- mAb and R-mAb could be detected separately using subclass-specific secondary Abs.

Effective cloning and IgG subclass switching of a widely used monoclonal antibody

K28/43 mAb, a mouse mAb specific for the neural scaffolding protein PSD-95

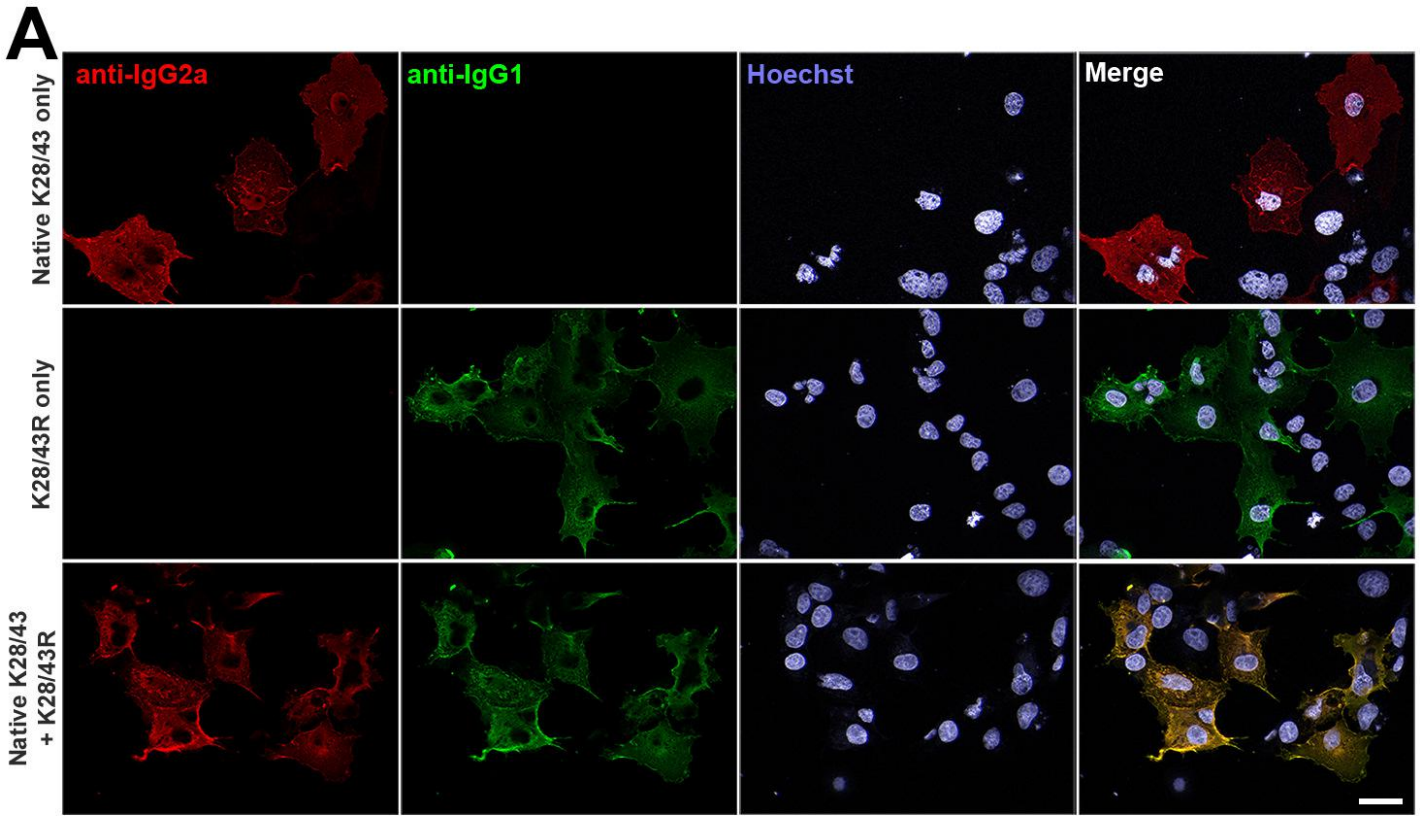

Validation of the K28/43R R-mAb in heterologous cells.

- The sample receiving only the native K28/43 hybridoma-generated mAb exhibited a signal corresponding to the IgG2a subclass-specific secondary Ab (red) with no detectable signal for the IgG1 subclass-specific secondary Ab (green).

- Conversely, labeling with the K28/43R R-mAb alone produced only an IgG1 subclass-specific green signal demonstrating a successful IgG subclass switch for the R-mAb

28/43 mAb is already of a less common IgG subclass (IgG2a)

They generated VL and VH domain cDNA fragments from the cryopreserved K28/43 hybridoma

Cloned them into the original P1316 plasmid that contains a mouse IgG1 CH domain

This indicates that both the mAb and R-mAb were recognizing the same target

Multiplex brain immunofluorescent labeling with subclass switched R-mAbs

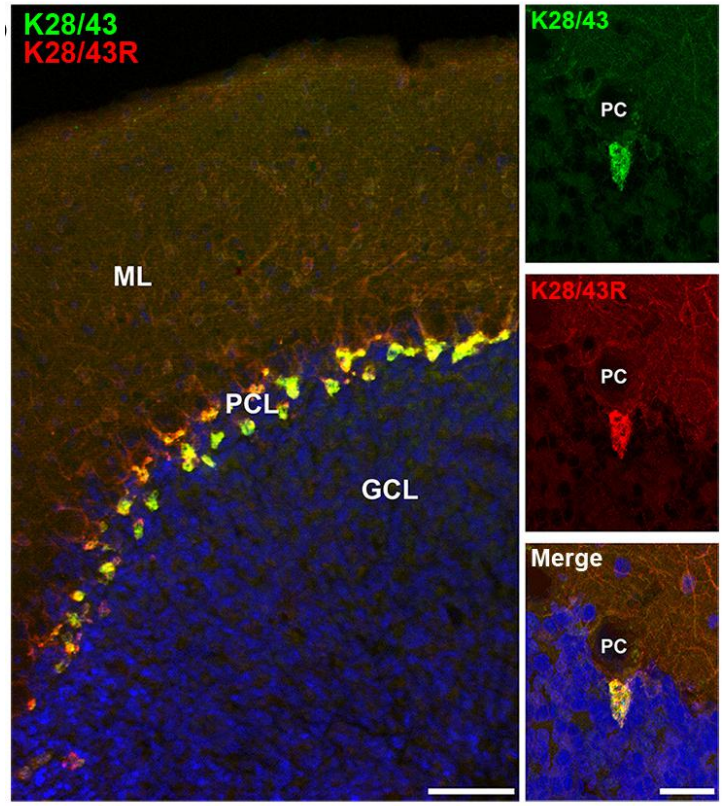

Validation of the K28/43R R-mAb in brain sections.

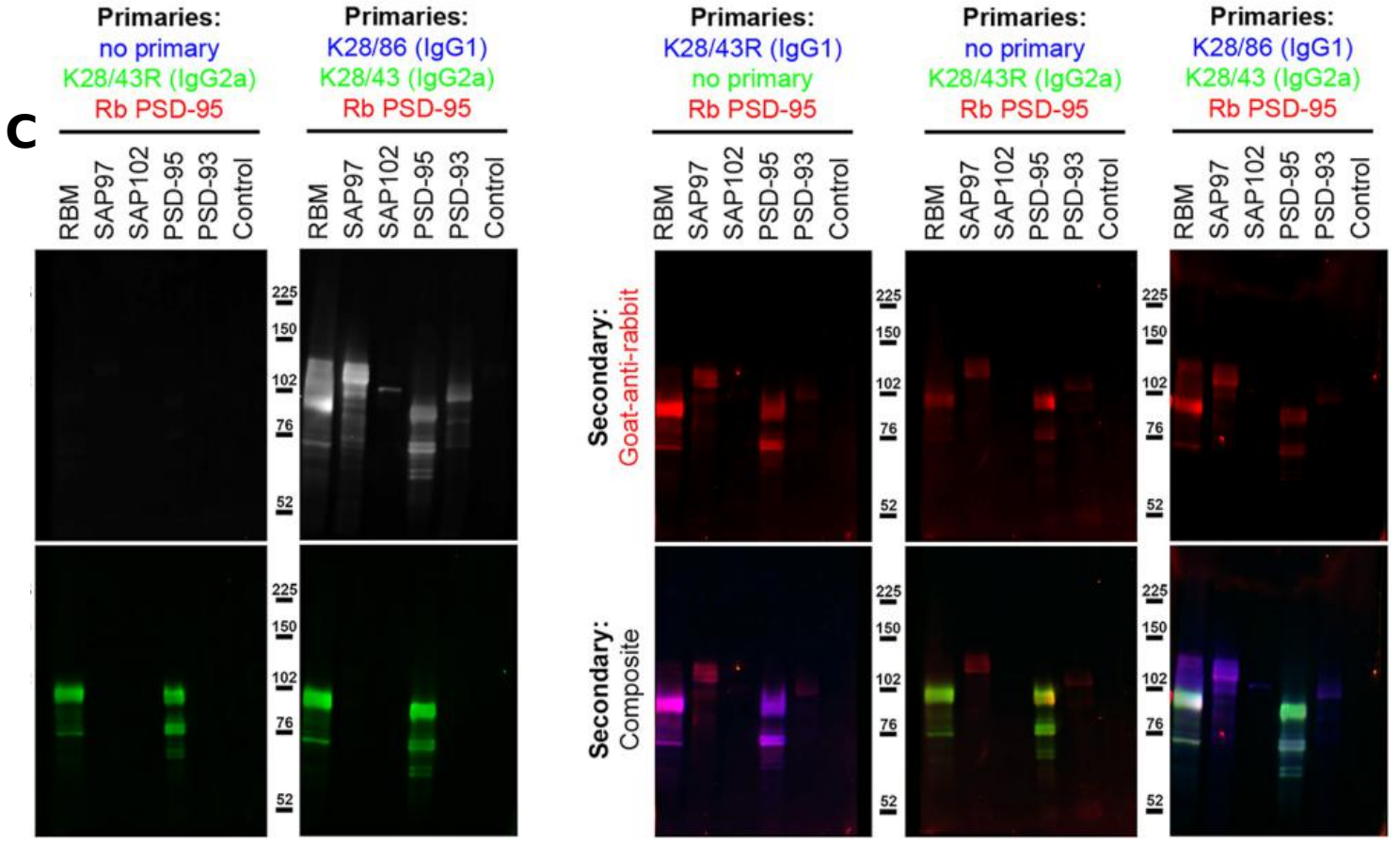

To confirm expression of these MAGUK proteins: immunoblots were probed with rabbit polyclonal anti-PSD-95 and with the hybridoma-generated K28/43 mAb (IgG2a) or a mAb that recognizes all mammalian MAGUK proteins mAb (K28/86; IgG1)

Both the IgG1 and IgG2a subclass isoforms of the K28/43R R-mAb gave identical immunolabeling patterns against samples from rat brain and COS-1 cells overexpressing PSD-95.

https://www.addgene.org/James_Trimmer/ → Possibility to generate and validate subclass-switched R-mAbs that recapitulate the immunolabeling characteristics of the native mAbs.

Multiplex brain immunofluorescent labeling with subclass switchedR-mAbs

Benefit of subclass switching R-mAbs:

--> ability to perform multiplex immunolabeling not previously possible due to IgG subclass conflicts

K65/35 an IgG1 subclass antibody directed to Nav channels
--> switch to IgG2a

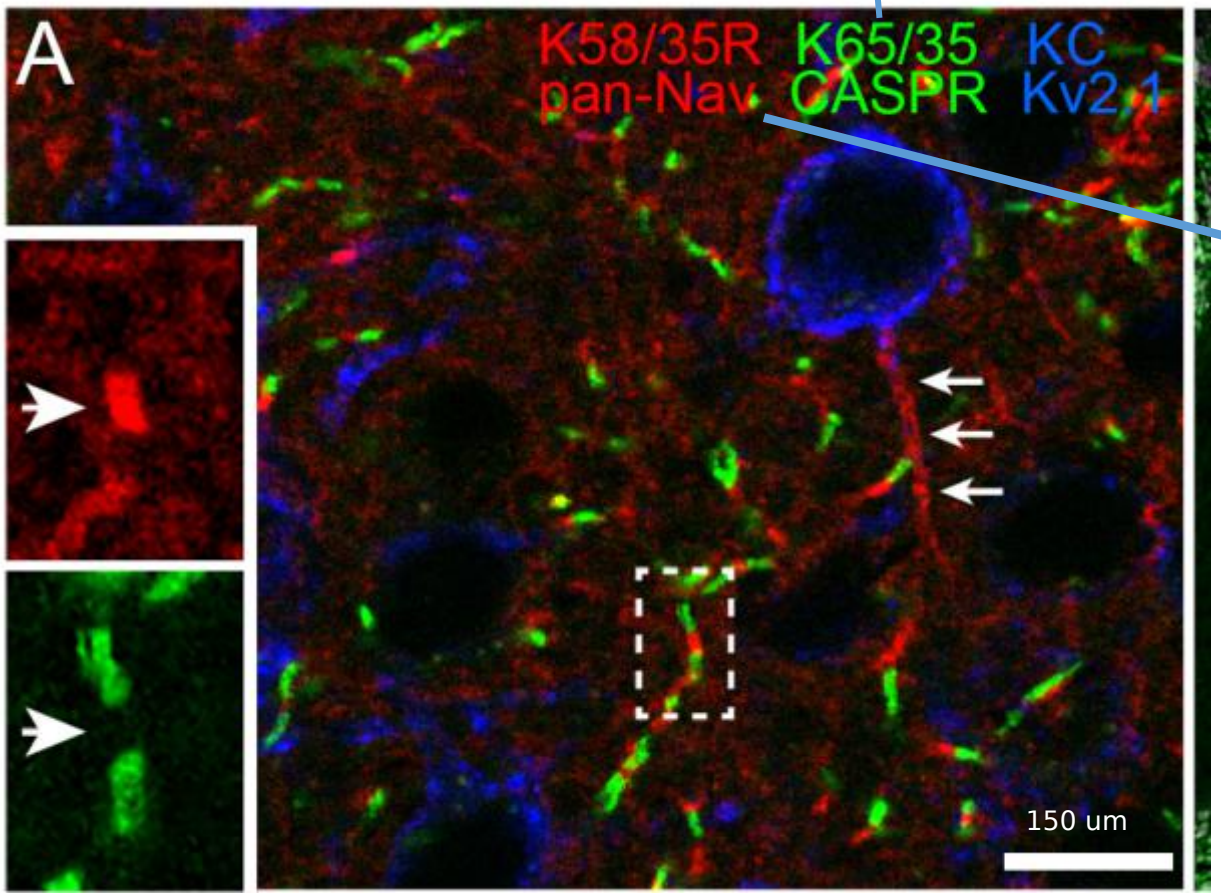

IgG2aR-mAb derived from pan-voltage-gated sodium channel or ‘pan-Nav channel’ IgG1mAb K58/35

Multiplex brain immunofluorescent labeling with subclass switchedR-mAbs

Benefit of subclass switching R-mAbs:

--> ability to perform multiplex immunolabeling not previously possible due to IgG subclass conflicts

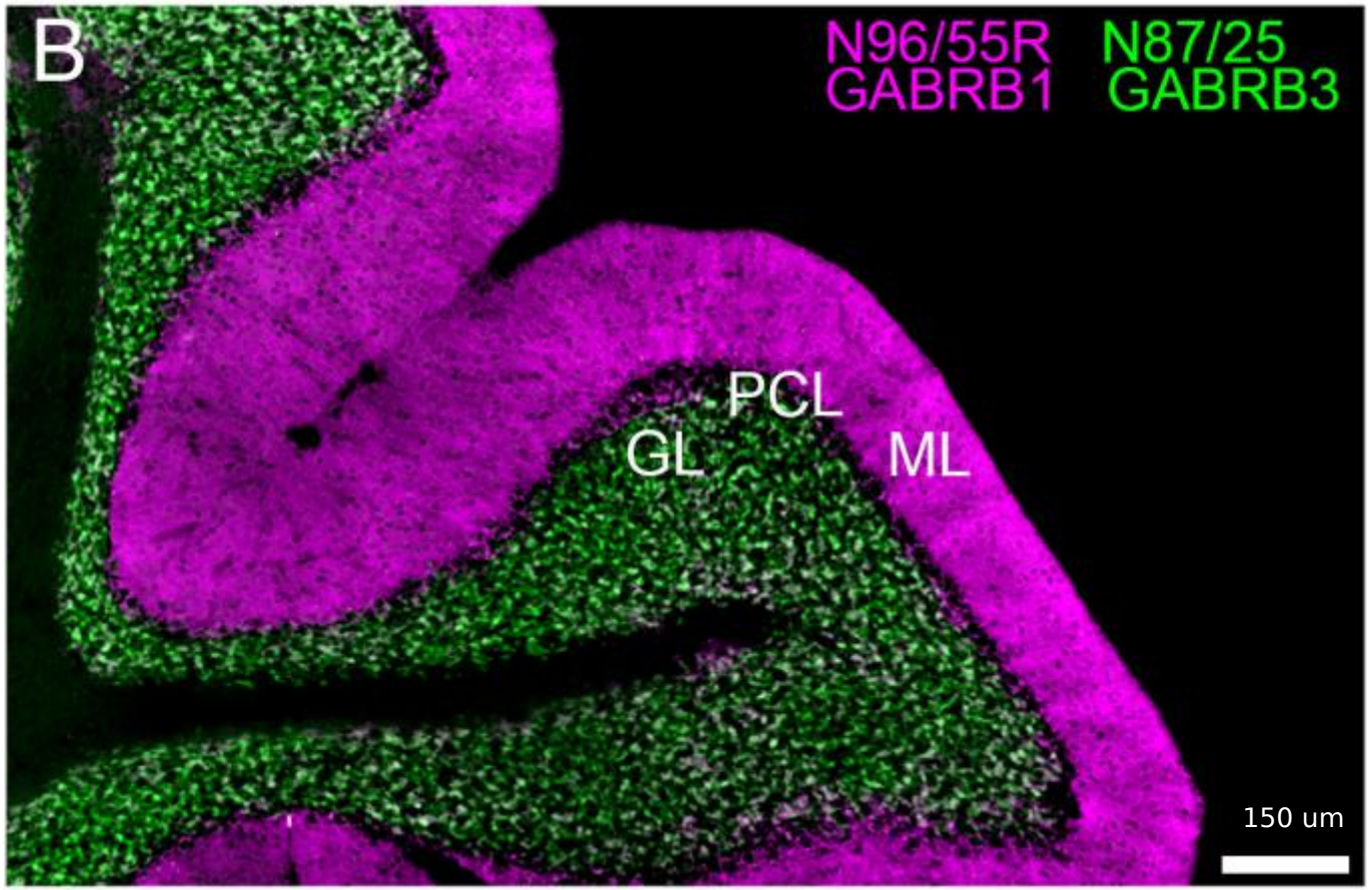

switching the N96/55 mAb to the IgG2a N96/55R R-mAb

=

simultaneous detection of GABA-A receptor b1 and b3 subunits.

Multiplex brain immunofluorescent labeling with subclass switchedR-mAbs

IgG2a, red IgG1, green

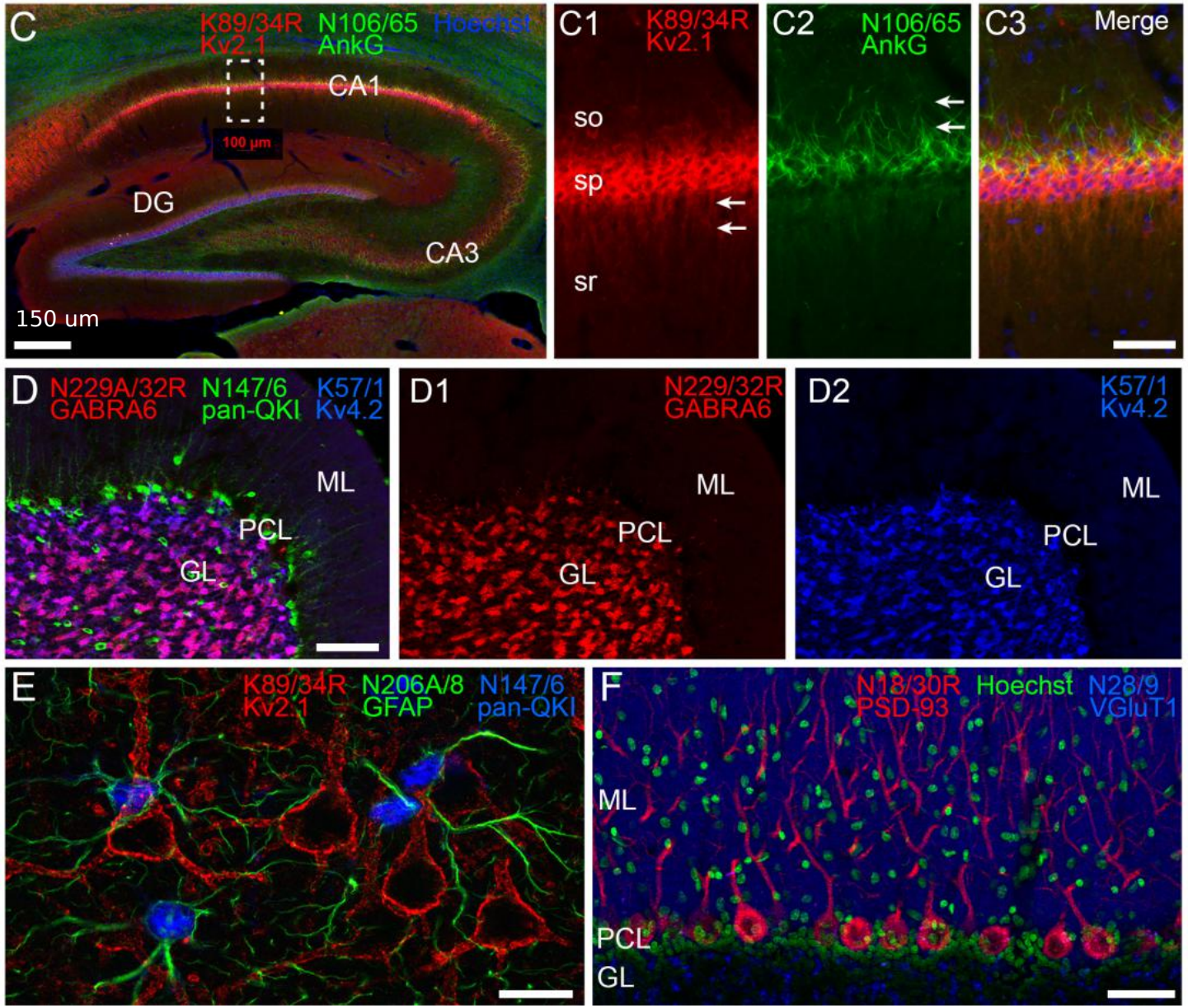

- K89/34R R-mAb (IgG2a, red), specific for the Kv2.1 channel highly expressed in plasma membrane of the cell body and proximal dendrites

N106/65 (green), an IgG1 mAb specific for AnkyrinG

- Subclass switching N229A/32 (IgG1, GABA-AR a6) to IgG2a, allows comparison with Kv4.2 potassium channel (K57/1, IgG1) in the cerebellum where both are highly expressed in the granule cell layer

- pan-QKI (N147/6, IgG2b, blue) =olygodendrocytes

GFAP (N206A/8, IgG1, green)= astrocytes

Multiplex labeling for the neuron-specific Kv2.1 channel, using subclass-switched K89/34R (IgG2a, red) confirms non-neuronal localization of both proteins.

- Excitatory presynaptic terminal marker VGluT1 mAb N28/9 (IgG1, blue), which exhibits robust labeling of parallel fiber synapses

Recovery of functional R-mAbs from a non-viable hybridoma

Is it possible to generate functional R-mAbs from hybridoma cell lines that are no longer viable in cell culture?

- They took Hybridoma cell line that produced the D3/71 mAb (for special binding site of Kv2.1 voltage-gated K+ channel).
- Attempted to resuscitate this cryopreserved hybridoma cell line over 20 years after it was cryopreserved, the D3/71 hybridoma cells were no longer viable.

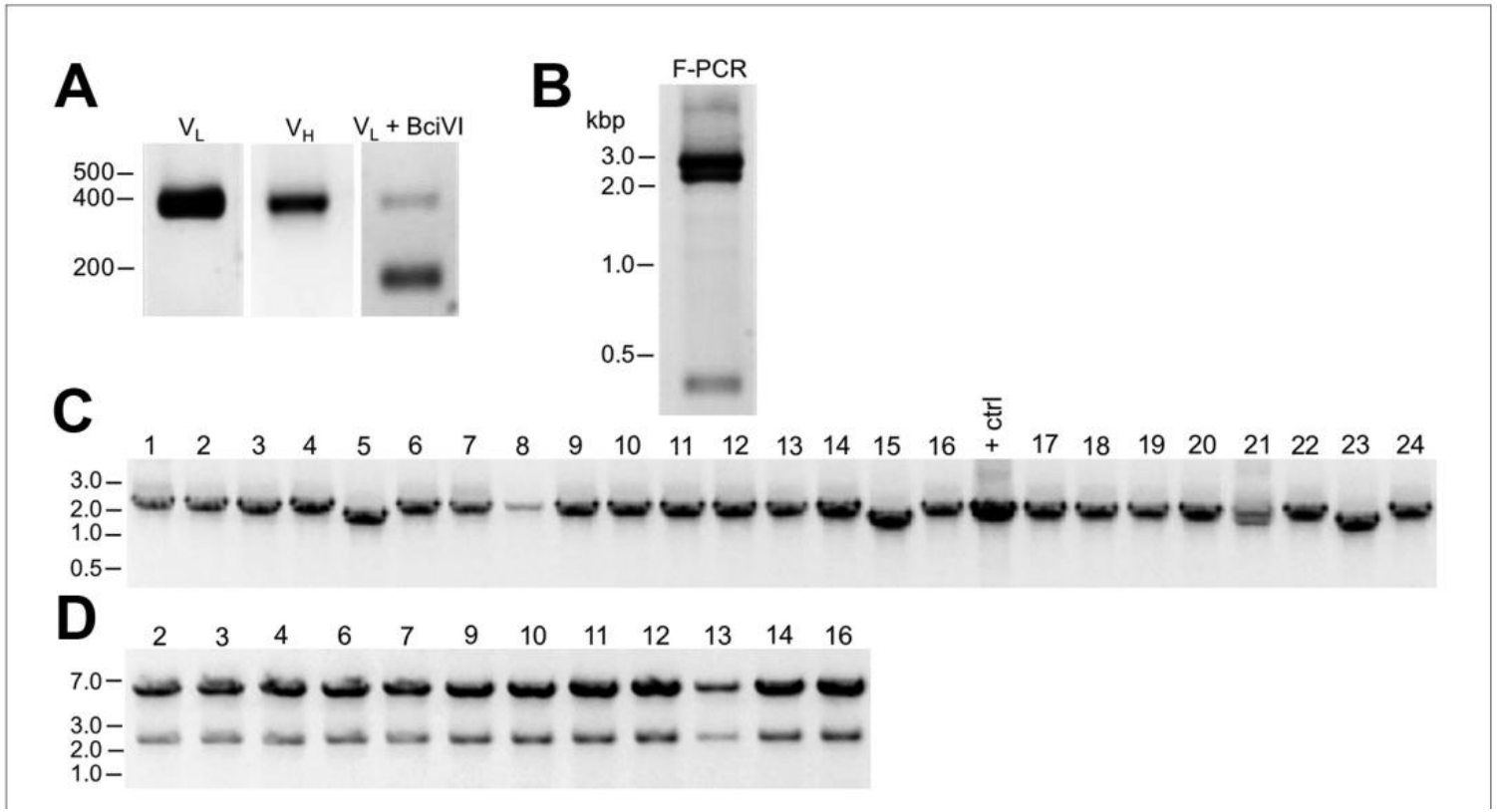

Colony PCR samples of transformants from the of D3/71 R-mAb project

Restriction enzyme digestion of D3/71 plasmid DNA with NotI and AscI.

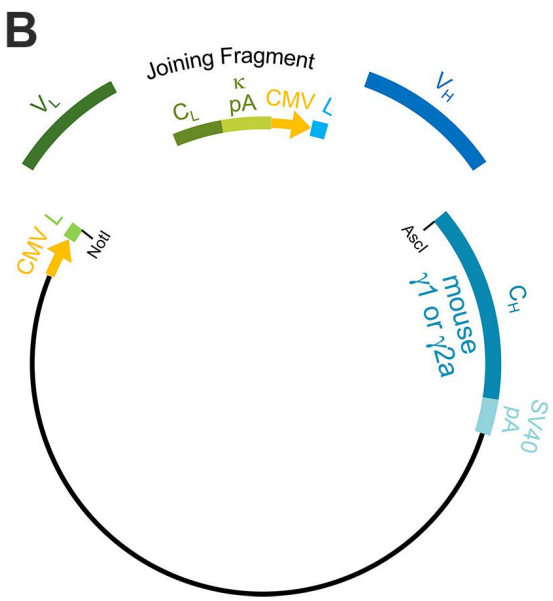

Recovery of functional R-mAbs from a non-viable hybridoma

distinct native anti-Kv2.1 IgG1 mAb K89/34

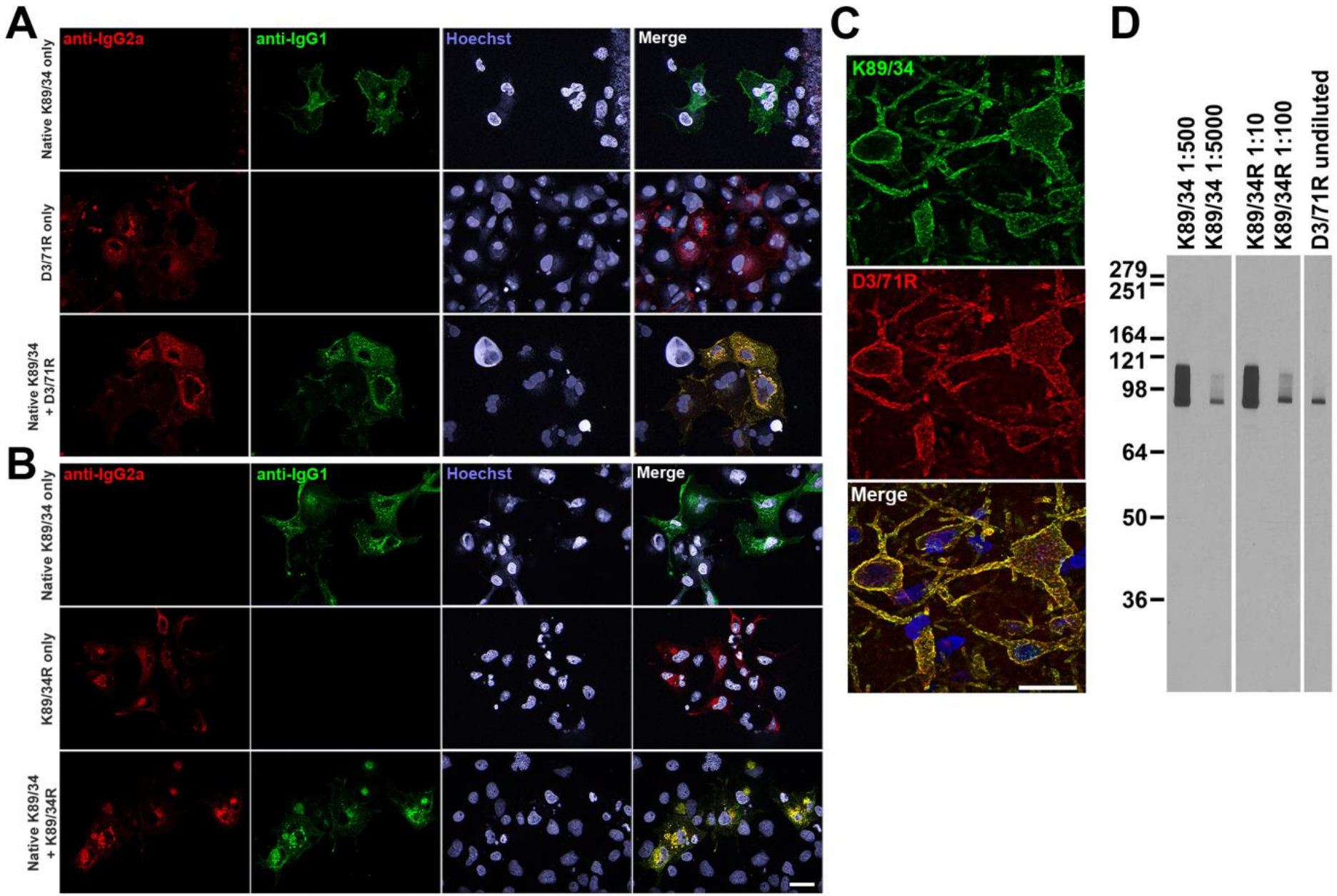

Outlook

Novel R-mAb generation and validation procedure that can be used to generate a valuable R-mAb resource by converting a library of widely used mouse mAbs into recombinant reagents.

- R-mAbs were produced in the culture medium from transiently transfected cells under standard mammalian cell culture conditions in sufficient quantities that they did not require purification for effective use in IB, ICC, and IHC assays.

- The efficiency of the process was further enhanced by **restriction digest of VL PCR products to eliminate the derived aberrant light chain.**

- The use of mouse mAbs of different IgG subclasses in combination with anti-mouse IgG subclass-specific secondary antibodies for simultaneous multiplex immunolabeling.

- The optimal utility of mouse mAbs in research and diagnostics is limited by the preponderance of IgG1 mAbs.

--> they have enhanced the flexibility of a substantial fraction of an existing library of widely used mouse mAbs by converting them to subclass-switched R-mAbs without altering target binding specificity.

- We show using mixtures ofmAbs and R-mAb that we can obtain **effective simultaneous multiplex labeling for combinations that were previously unattainable due to conflicting IgG subclass.**

Introduction_paper #2

- Histopathology is among the most important and widely used methods for diagnosing human disease and studying the development of multicellular organisms.
- The potential of IHC to aid in diagnosis and prioritization of therapy is well established.
- However, IHC has some limitations: imaging multiple antigens usually involves the analysis of sequential tissue slices or harsh stripping protocols.

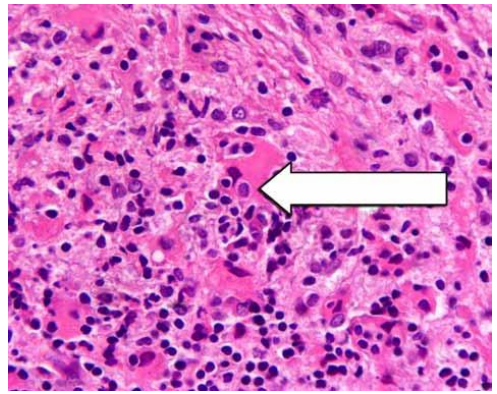

Different dyes and antibodies stainings to look at single cells at the same time

Some methods for multilabelling

FISSEQ

SOLiD

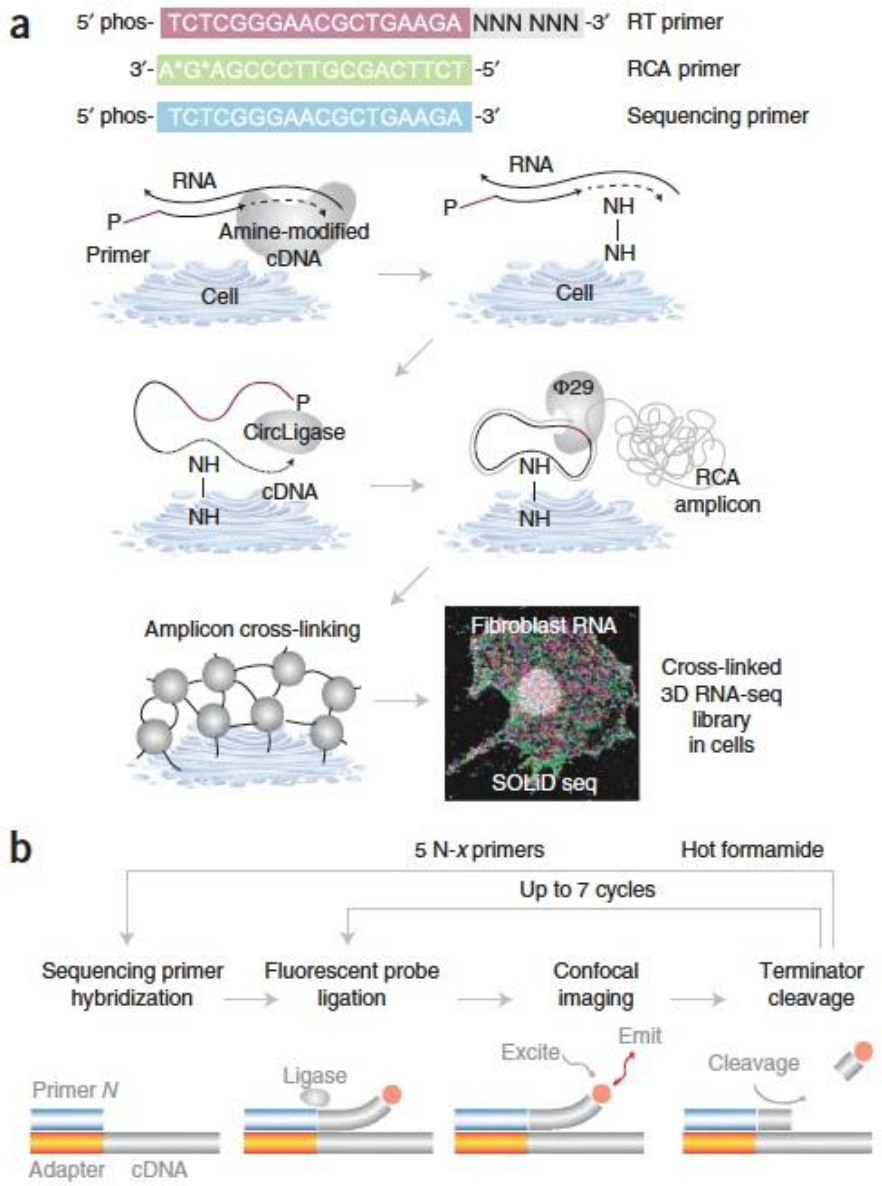

(Lee et al., 2014)

Some methods for multilabelling

Multiplexed ion beam imaging-IMIB

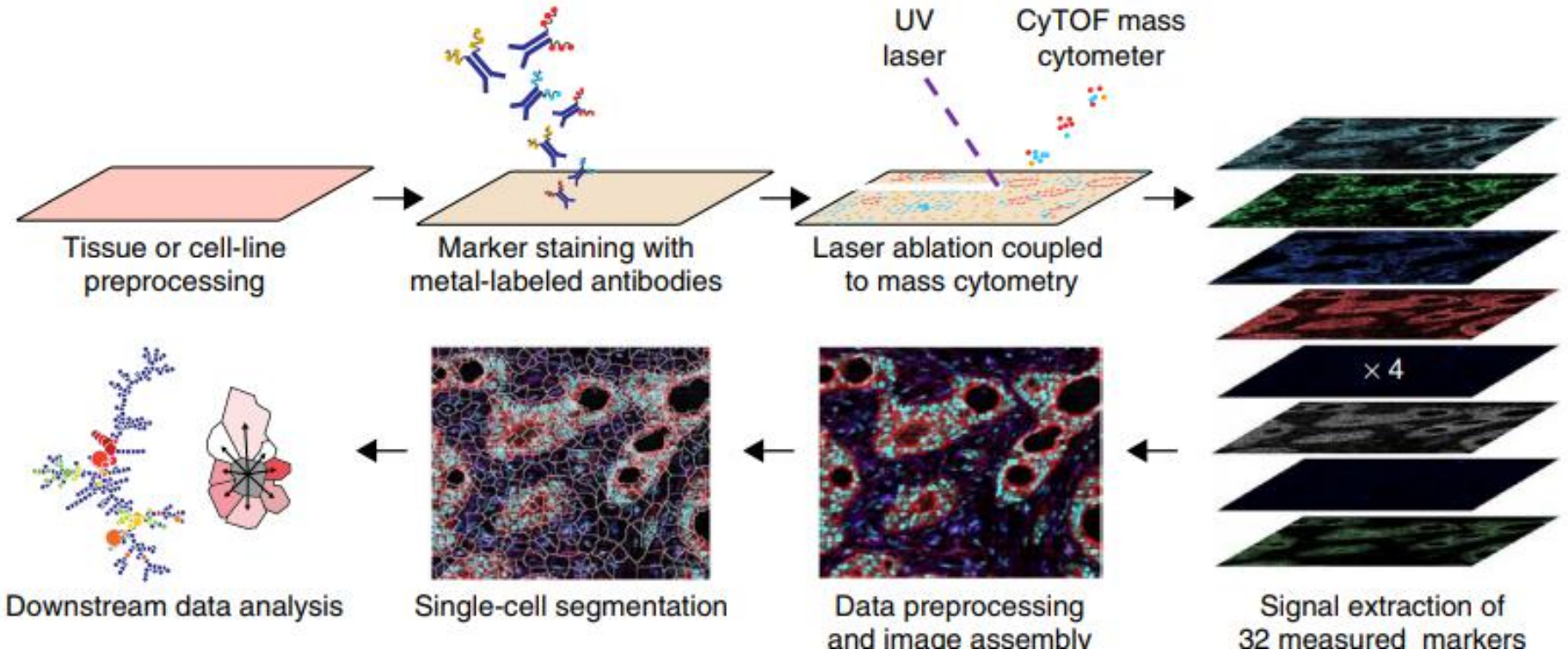

It measures the abundance of metal isotopes tagged to antibodies, and amplification is achieved by a polymeric metal-chelating reagent or metal nanoparticles

(Giesen et al., 2014)

LIMITATIONS

- They require specialized instrumentation and consumables.
- Laser ablation of samples, such as MIBI, inherently have a lower resolution than optical imaging.

OBJECTIVES for future immunolabeling techniques

(i) minimize the requirement for specialized instruments and costly, proprietary reagents.

(ii) work with conventionally prepared FFPE tissue specimens collected in clinical practice and research settings.

(iii) enable imaging of ca. 50 antigens at subcellular resolution across a wide range of cell and tumor types.

(iv) collect data with sufficient throughput that large specimens (several square centimeters) can be imaged and analyzed.

(v) generate high-resolution data typical of optical microscopy.

(vi) allow investigators to customize the antibody mix to specific questions or tissue types.

Paper #2_Tissue-based cyclic immunofluorescence (t-CyCIF)

eLIFE elifesciences.org

TOOLS AND RESOURCES

Highly multiplexed immunofluorescence imaging of human tissues and tumors using t-CyCIF and conventional optical microscopes

Jia-Ren Lin[1,2†], Benjamin Izar[1,2,3,4†], Shu Wang[1,5], Clarence Yapp[1], Shaolin Mei[1,3], Parin M Shah[3], Sandro Santagata[1,2,6,7], Peter K Sorger[1,2*]

[1]Laboratory of Systems Pharmacology, Harvard Medical School, Boston, United States; [2]Ludwig Center for Cancer Research at Harvard, Harvard Medical School, Boston, United States; [3]Department of Medical Oncology, Dana-Farber Cancer Institute, Boston, United States; [4]Broad Institute of MIT and Harvard, Cambridge, United States; [5]Harvard Graduate Program in Biophysics, Harvard University, Cambridge, United States; [6]Department of Pathology, Brigham and Women's Hospital, Harvard Medical School, Boston, United States; [7]Department of Oncologic Pathology, Dana-Farber Cancer Institute, Boston, United States

Published: 11th July 2018

t-CyCIF enables multiplexed imaging of FFPE tissue and tumor specimens at subcellular resolution

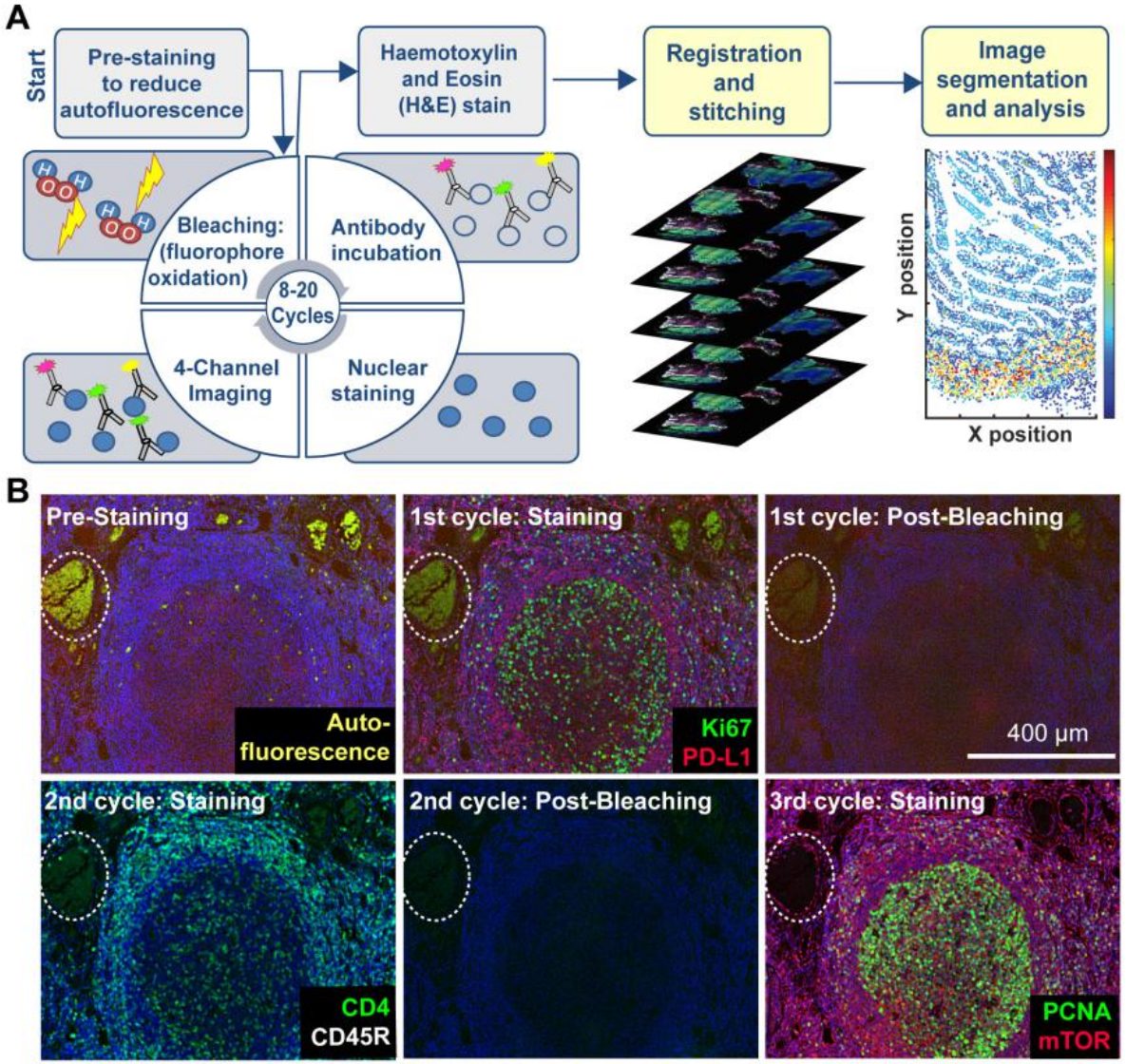

(i) immuno-staining with antibodies against protein antigens (three antigens per cycle)

(ii) staining with a DNA dye (commonly Hoechst 33342) to mark nuclei and facilitate image registration across cycles

(iii) four-channel imaging at low- and high-magnification

(iv) fluorophore bleaching followed by a wash step and then another round of immunostaining.

Note: The signal-to-noise ratio often increases with cycle number due to progressive reductions in background intensity over the course of multiple rounds of fluorophore bleaching.

Microscopes used in this study and their properties.

Instrument	Type	Objective	Field of view	Nominal Resolution*
RareCyte Cytefinder	Slide Scanner	10X/0.3 NA	1.6 × 1.4 mm	1.06 μm
		20X/0.8NA	0.8 × 0.7 mm	0.40 μm
		40X/0.6 NA	0.42 × 0.35 mm	0.53 μm
GE INCell Analyzer 6000	Confocal	60X/0.95 NA	0.22 × 0.22 mm	0.21 μm
GE OMX Blaze	Structured Illumination Microscope	60 × 1.42 NA	0.08 × 0.08 mm	0.11 μm

Different tradeoff between data acquisition time, image resolution and sensitivity

Greater resolution (a higher numerical aperture objective lens) typically corresponds to a smaller field of view and thus, longer acquisition time for large specimens.

Multi-scale imaging of t-CyCIF metastatic melanoma specimens

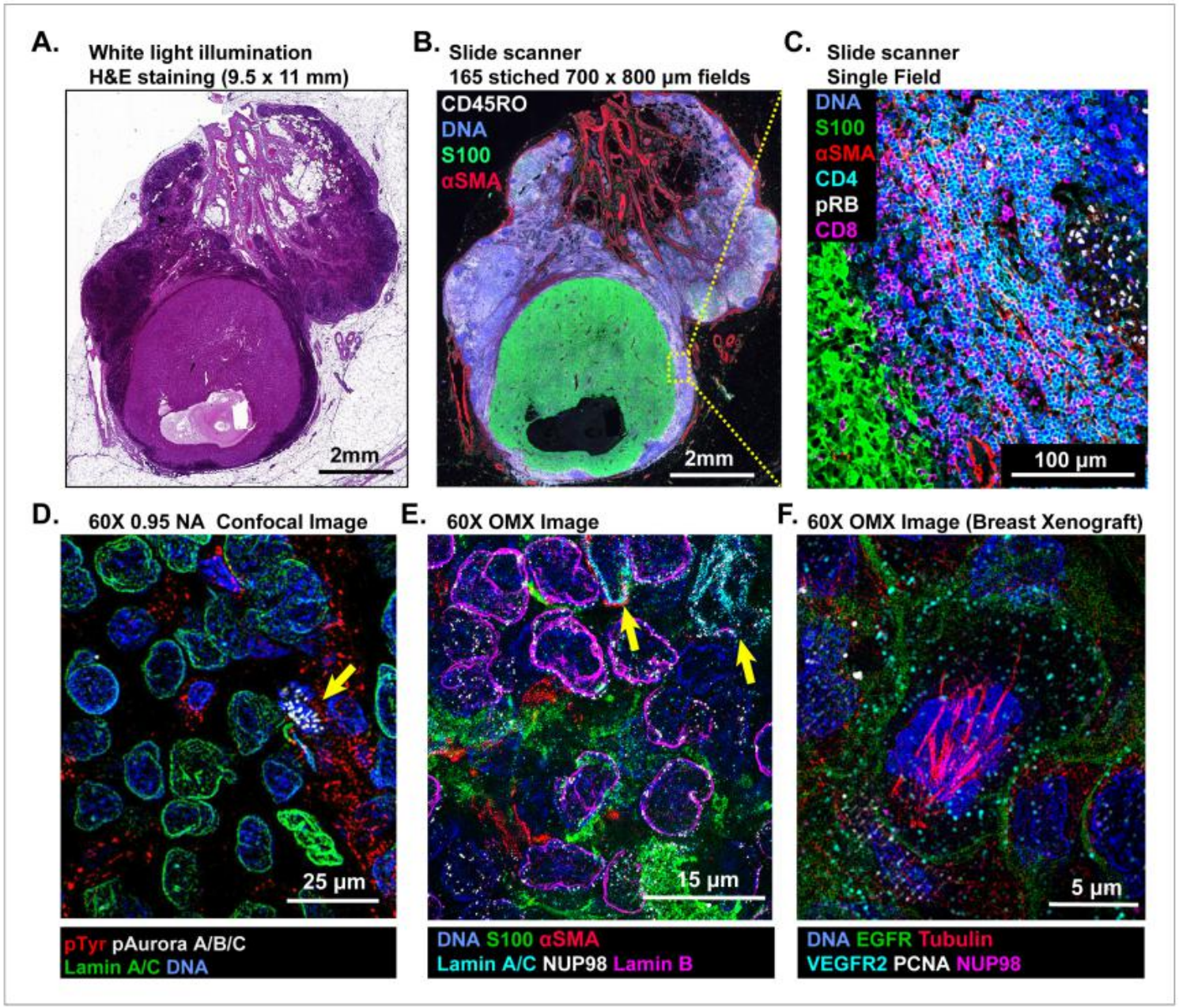

CyCIF images have readily interpretable features at the scale of:

- an entire tumor
- individual tumor cells
- subcellular structures.

t-CyCIF imaging of normal tissues.

A

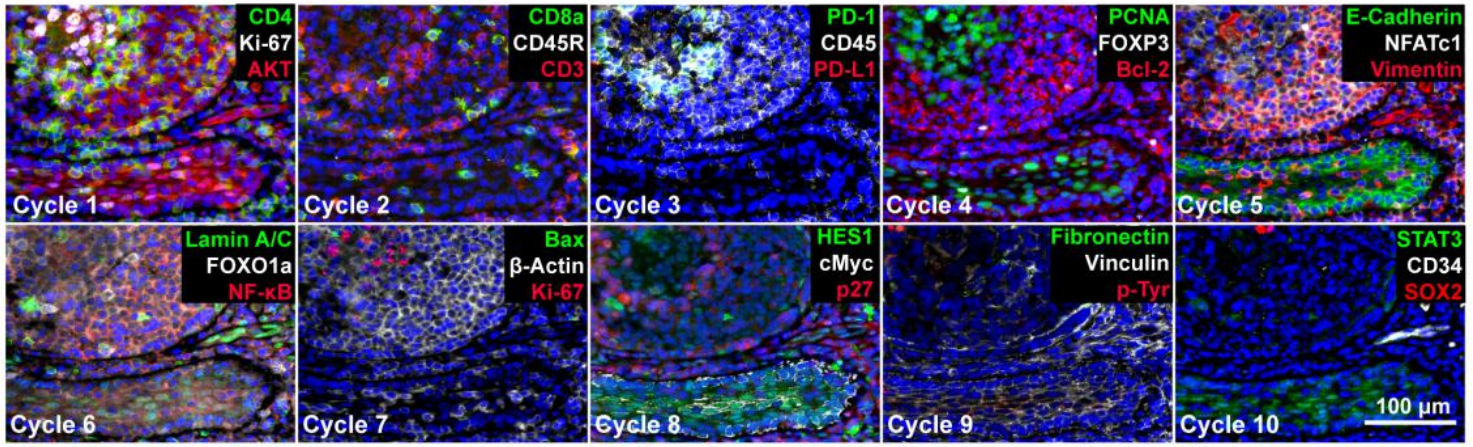

(A) Selected images of a tonsil specimen subjected to 10-cycle t-CyCIF to demonstrate

- Tissue
- Cellular
- Subcellular

localization of tissue and immune markers

B

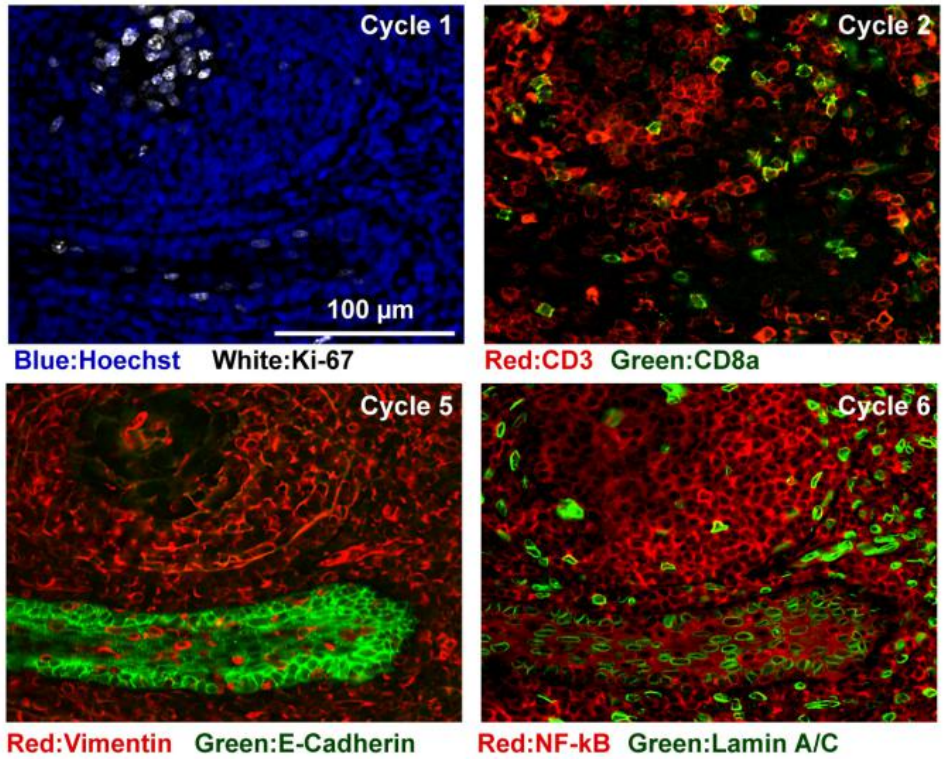

(B) Selected cycles from (A) demonstrating sub-nuclear features:

- Ki67 staining, (cycle 1)
- immune cell distribution (cycle 2)
- structural proteins (E-Cadherin and Vimentin, (cycle 5)
- nuclear vs. cytosolic localization of transcription factors (NF-kB, cycle 6).

t-CyCIF imaging of normal tissues.

C

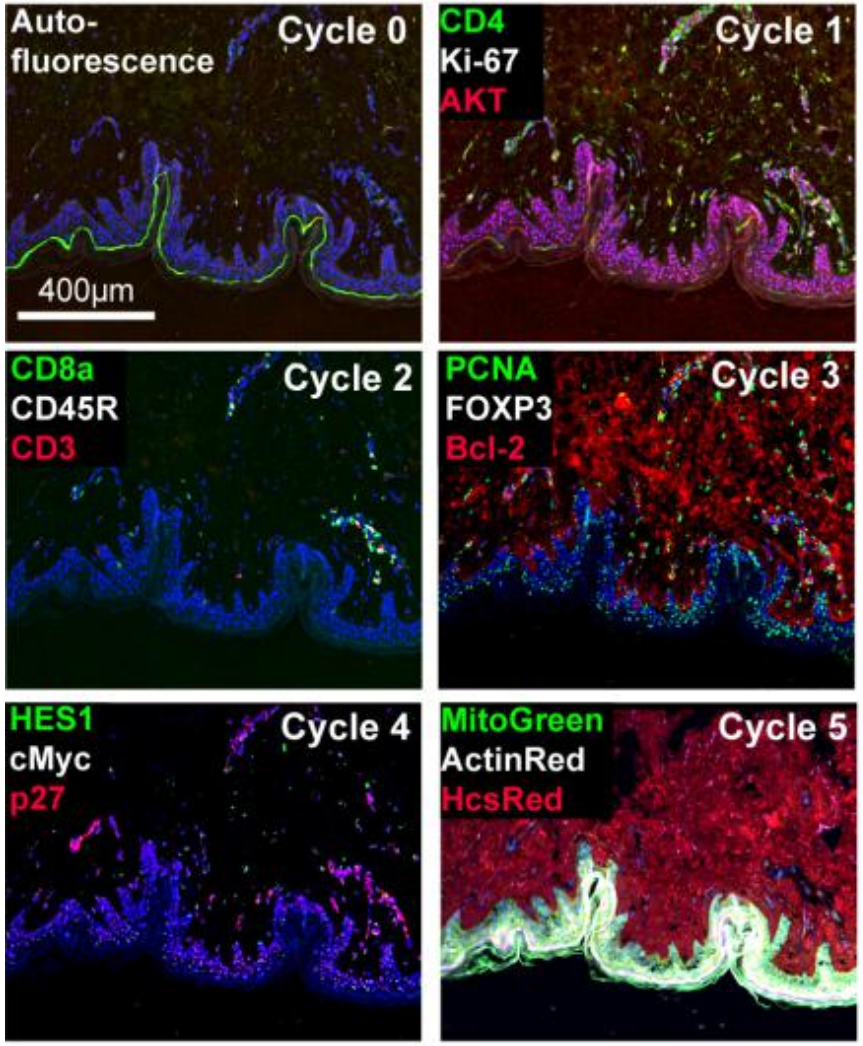

(C) Five-cycle t-CyCIF of human skin to show:

- the tight localization of some autofluorescence signals (Cycle 0),
- the elimination of these signals after pre-staining (Cycle 1),
- the dispersal of rare cell types within a complex layered tissue

Fluorophore inactivation, cycle count and tissue integrity

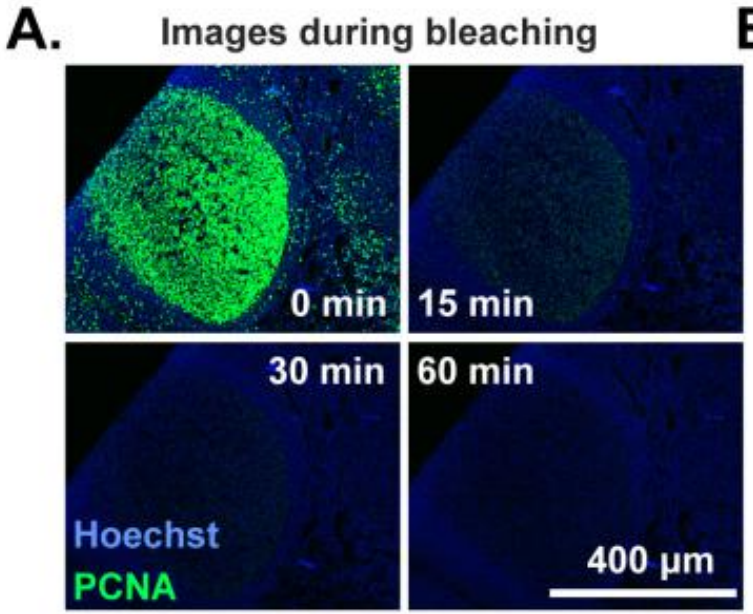

PCNA=proliferating cell nuclear antigen

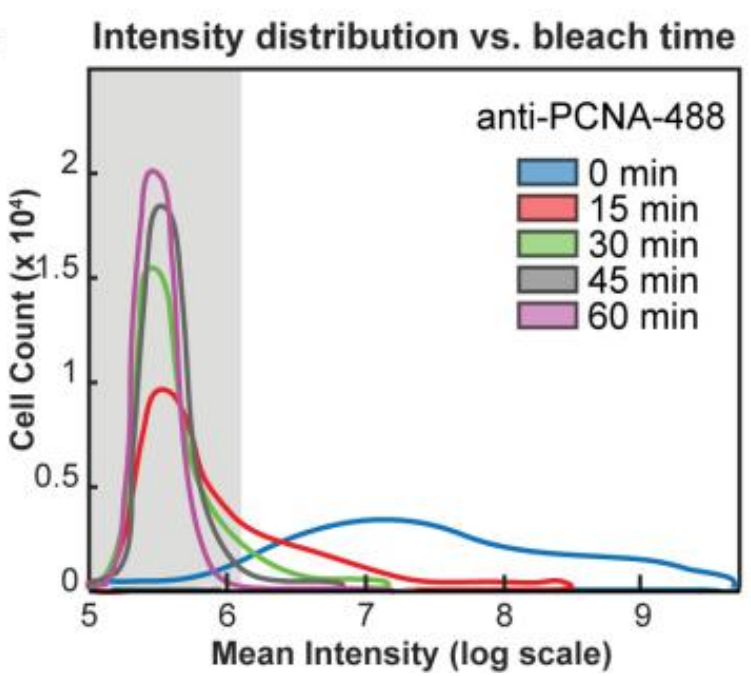

The efficiency of fluorophore inactivation by hydrogen peroxide, light and high pH varies with fluorophore but only minimally with the antibody to which the fluorophore is coupled.

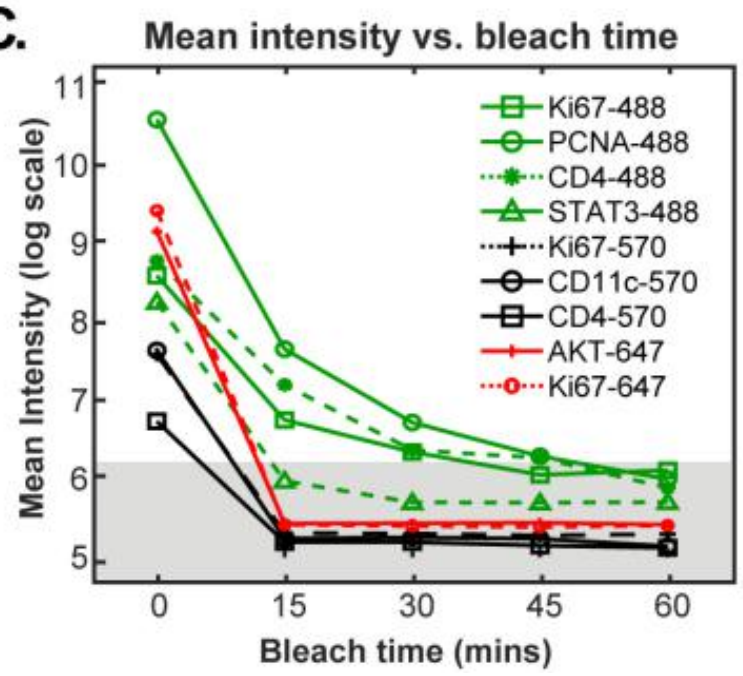

Incubation of specimens in bleaching conditions for 60 is sufficient to reduce fluorescence intensity by 10 2 to 10 3 -fold

-> Alexa Fluor 488 is inactivated more slowly than Alexa Fluor 570 or 647

Fluorophore inactivation, cycle count and tissue integrity

The primary limitation on the number of t-CyCIF cycles that can be performed is the integrity of the tissue:
--> some tissues samples are physically more robust and can withstand more staining and washing procedures than others

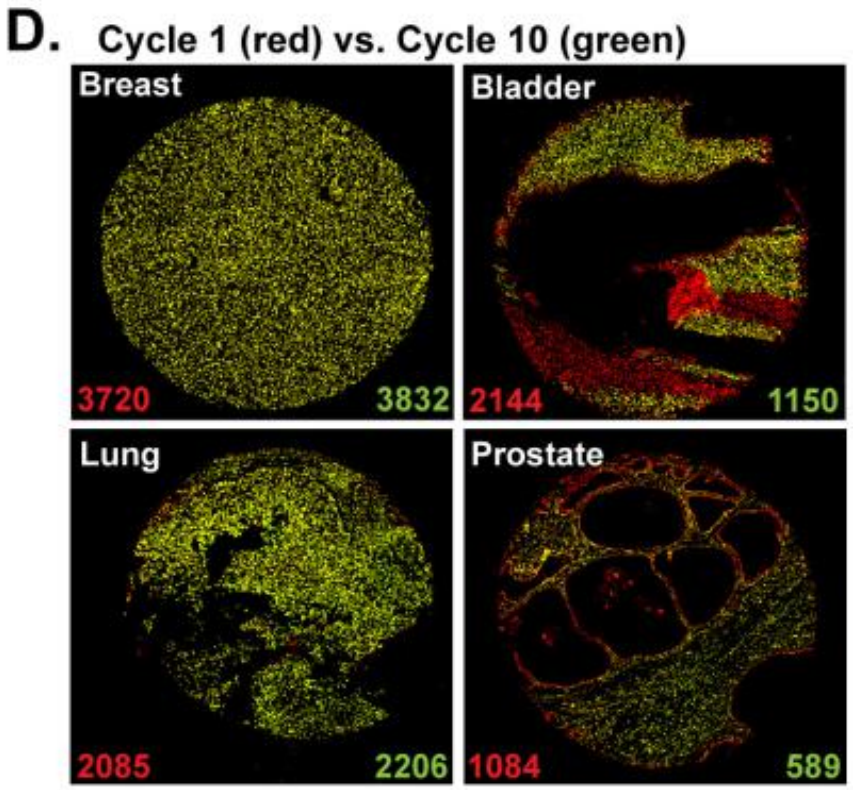

Cell loss is often uneven across samples, preferentially affecting regions of tissue with low cellularity.

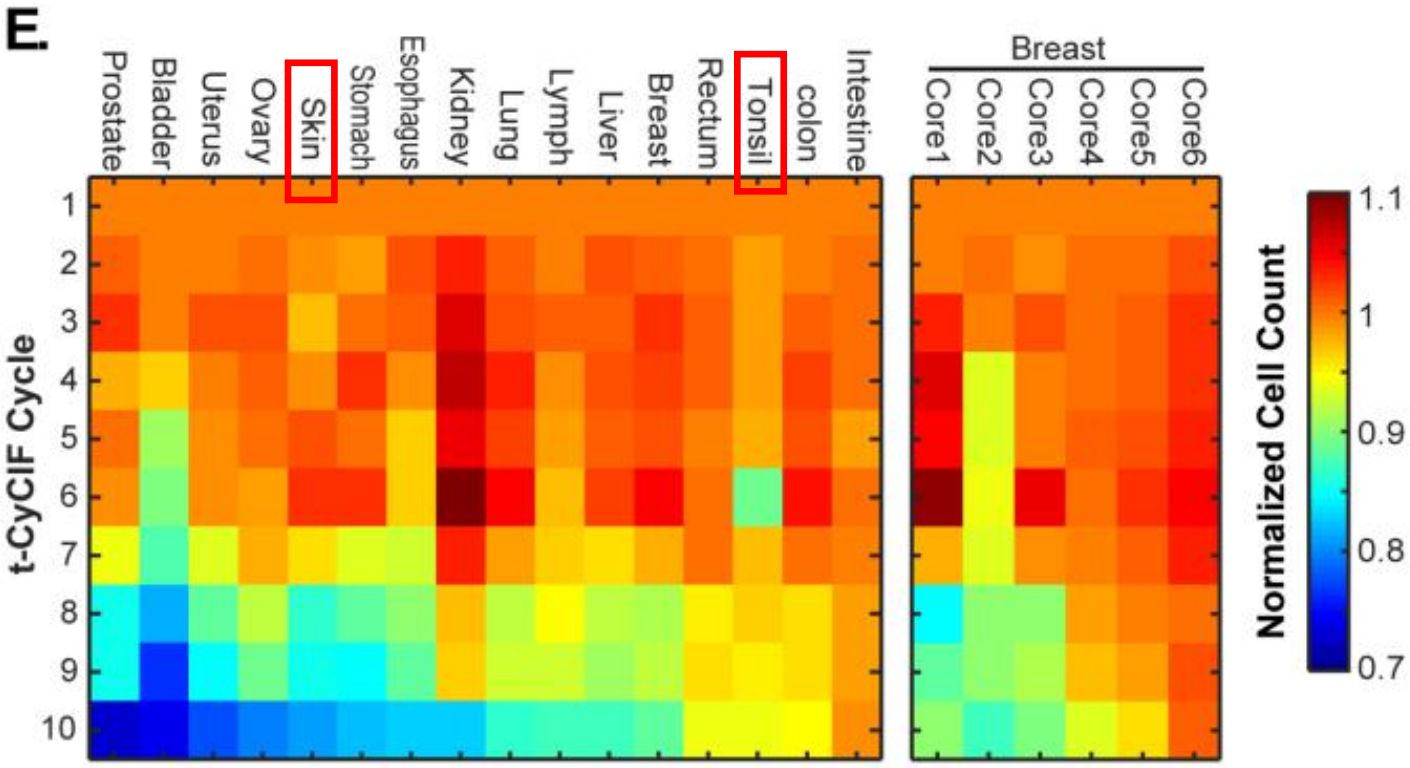

Cell loss varied with tissue type and, within a single tissue type, from core to core.

Fluorophore inactivation, cycle count and tissue integrity

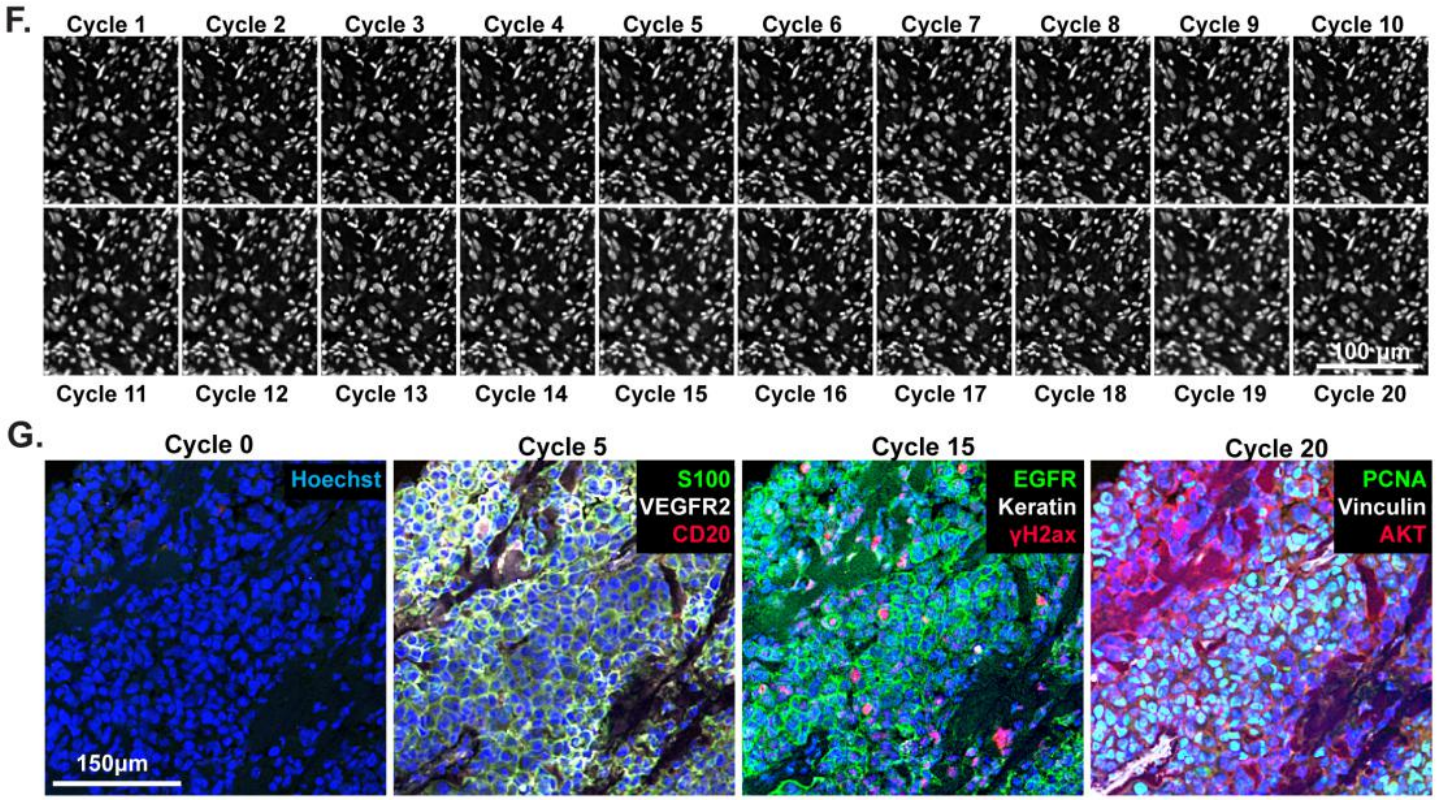

(F) Nuclear staining of a melanoma specimen subjected to 20 cycles of t-CyCIF emphasizes the preservation of tissue integrity.

(G) Selected images of the specimen in (F) from cycles 0, 5, 15 and 20.

- t-CyCIF is compatible with multiple normal tissues and tumor types
- some tissues and/or specimens can be subjected to more cycles than others
- cellularity: samples in which cells are very sparse tend to be more fragile.

Potential concern about cyclic immunofluorescence

- The process is relatively slow; each cycle takes 6–8 hr.
- Time could be saved by imaging fewer cells per sample, but the results strongly argue in favor of analyzing as large a fraction of each tissue specimen as possible.
- Data analysis and data interpretation remain more time consuming than data collection.

Impact of cycle number on immunogenicity

16-cycle t-CyCIF experiment in which the order of antibody addition was varied between two immediately adjacent tissue slices cut from the same tissue block

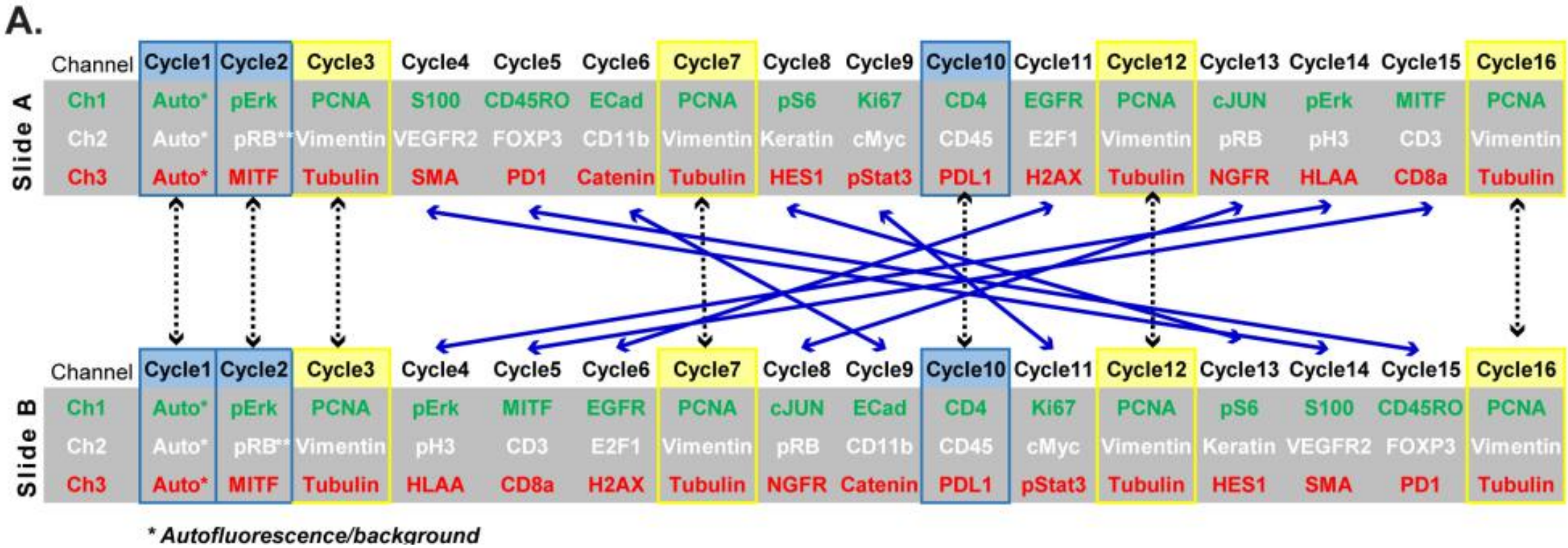

Judgment of:
(i) the repeatability of staining a single specimen using the same set of antibodies (Yellow highlight)

(ii) the similarity of staining between slides A and B (blue highlight)

(iii) the effect of swapping the order of antibody addition (cycle number) between slides A and B (blue lines).

Impact of cycle number on immunogenicity

(i) the repeatability of staining a single specimen using the same set of antibodies (Yellow highlight)

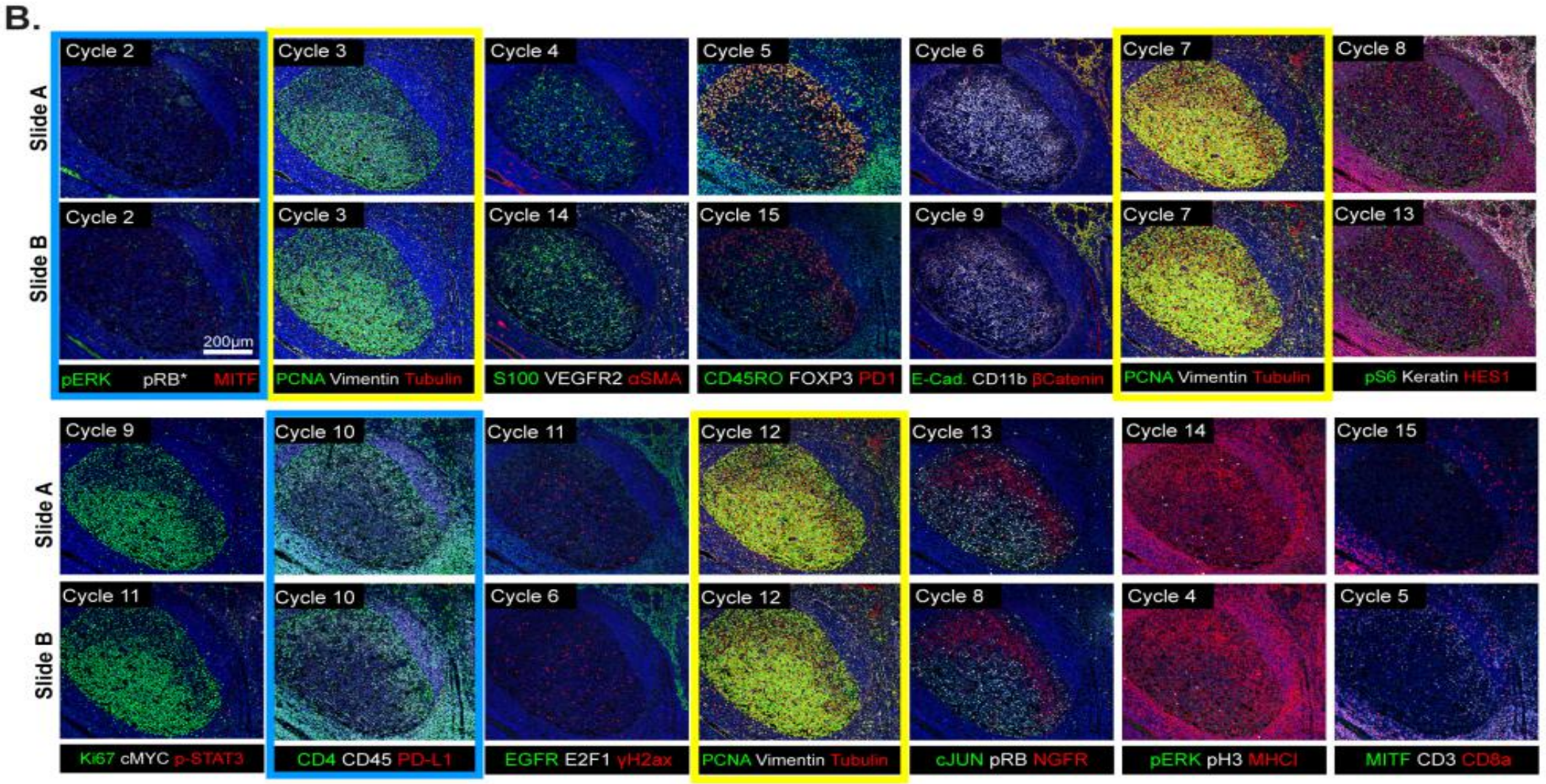

Tubulin, and to a lesser extent Vimentin, stained more intensely in later than in earlier t-CyCIF cycles

Impact of cycle number on immunogenicity

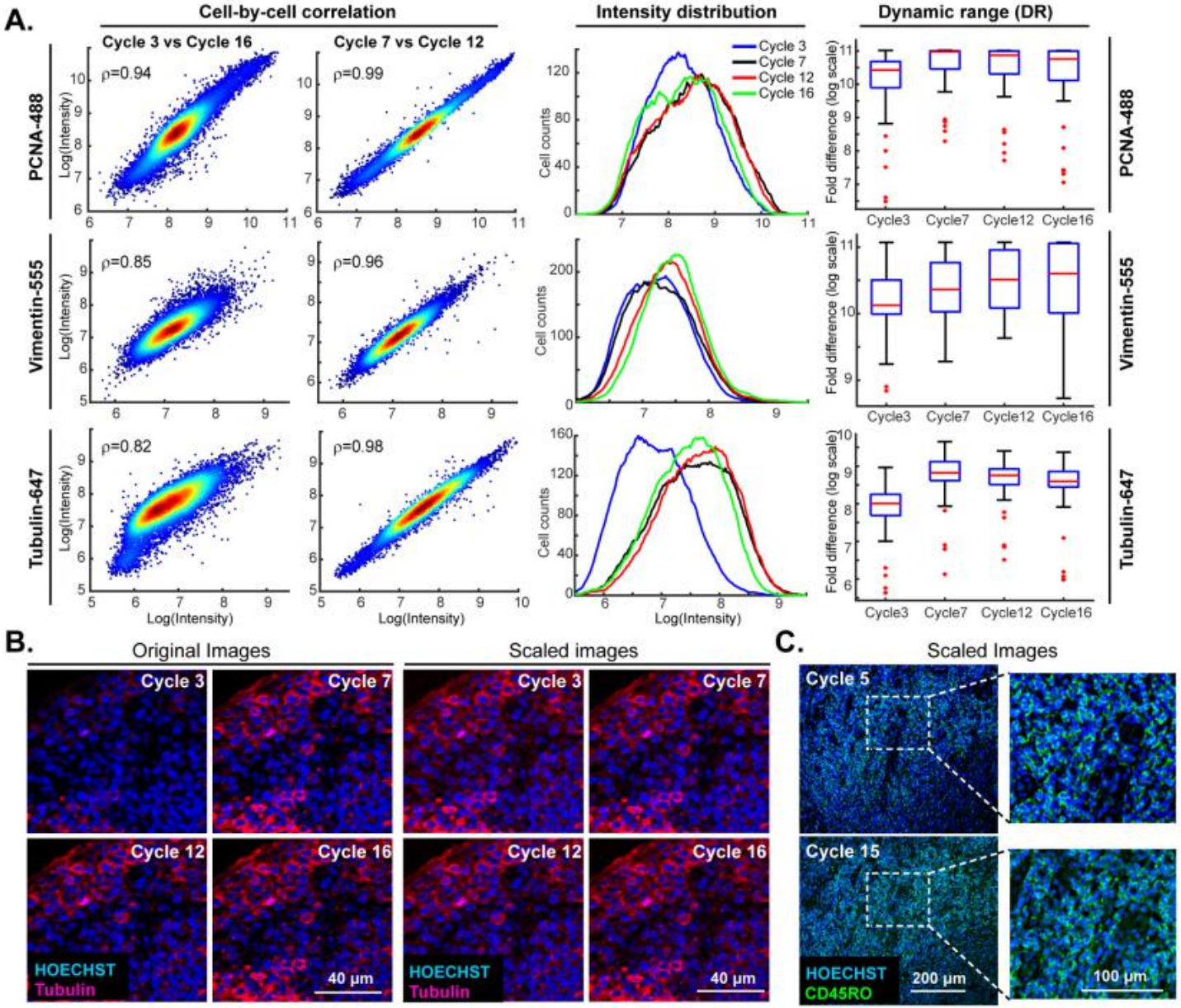

For at least a subset of antibodies, staining intensity increases rather than decreases with cycle number whereas background fluorescence falls.

DR= least 5% of pixels/ the most intense 5% of pixels frequently increases with cycle number

When images were scaled to equalize the intensity range (by histogram equalization):

- the staining patterns were indistinguishable across all cycles
- loss of cells or specific subcellular structures was not obviously a factor

Impact of cycle number on immunogenicity

(iii) the effect of swapping the order of antibody addition (cycle number) between slides A and B (blue lines).

D.

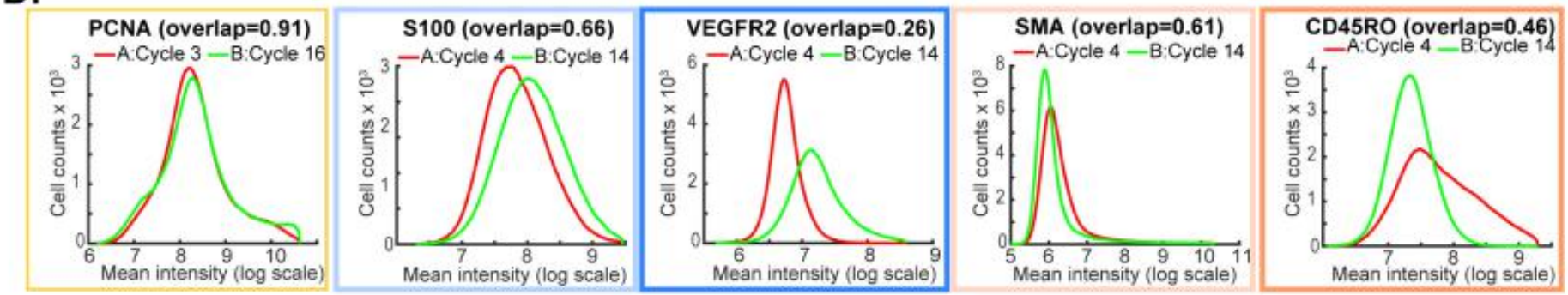

E.

Effect of cycle number	Overlap Integral	Antibodies
Little or no change	>0.8	PCNA, E2F1, gH2ax, cJUN, NGFR, pERK, HLAA, MITF, pS6, Keratin, beta- Catenin, E-Cadherin , FoxP3
Minor Increase with Cycle Number	0.6 to 0.8	S100, Ki67, pH3, Vimentin, pRB
Major increase with Cycle number	<0.6	VEGFR2, EGFR, CD8a, Tubulin
Minor Decrease with Cycle Number	0.6 to 0.8	CD11b, HES1, SMA
Major Decrease with Cycle Number	<0.6	CD45R0, PD1, CD3

F.

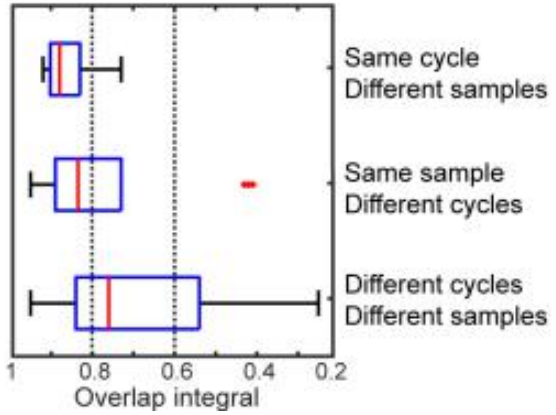

D) The overlap remained high for the majority of antibodies even when they were used in different cycles on slides A and B, but for some antibodies, signal intensity clearly increased or decreased with cycle number

E) In the case of eight antibodies for which the effect of cycle number was greatest, the overlap in intensity distributions was <0.6 as a consequence of both increases and decreases in staining intensity.

F) The repeatability of staining between two biological samples was highest when the antibodies were used in the same cycle on both samples.

- The reasons for **changes in staining intensity** with cycle number are not known, but the fact that the same changes were observed across multiple experiments (for any single antibody) suggests that they **arise not from irreproducibility of the t-CyCIF procedure but rather from changes in epitope accessibility.**

- Changes in staining intensity with cycle number are a concern for a subset of t-CyCIF antibodies, it should be possible to **minimize the problem by staining all samples in the same order**.

- Other approaches will also be important:

  - using calibration standards

  - identifying antibodies exhibiting the least variation with cycle number.

  - create a single high-plex antibody mixture and then stain all antigens in parallel (this approach is not compatible with t-CyCIF but is feasible using methods such as MIBI or CODEX (Angelo et al., 2014; Goltsev, 2017).

They finally observed that:

If eight or more unlabeled antibodies are added to a t-CyCIF experiment, the intensity of staining can fall, although the effect is smaller than observed with antibodies most sensitive to order of addition.

The construction of sequentially applied t-CyCIF antibody panels and of single high-plex mixtures will need optimization.

Analysis of large specimens by t-CyCIF

The capacity to image samples that are several square centimeters in area with t-CyCIF can facilitate the detection of signaling biomarker heterogeneity.

Eight-cycle t-CyCIF on a large 2X1.5 cm resection specimen that includes pancreatic ductal adenocarcinoma (PDAC) and adjacent normal pancreatic tissue and small intestine

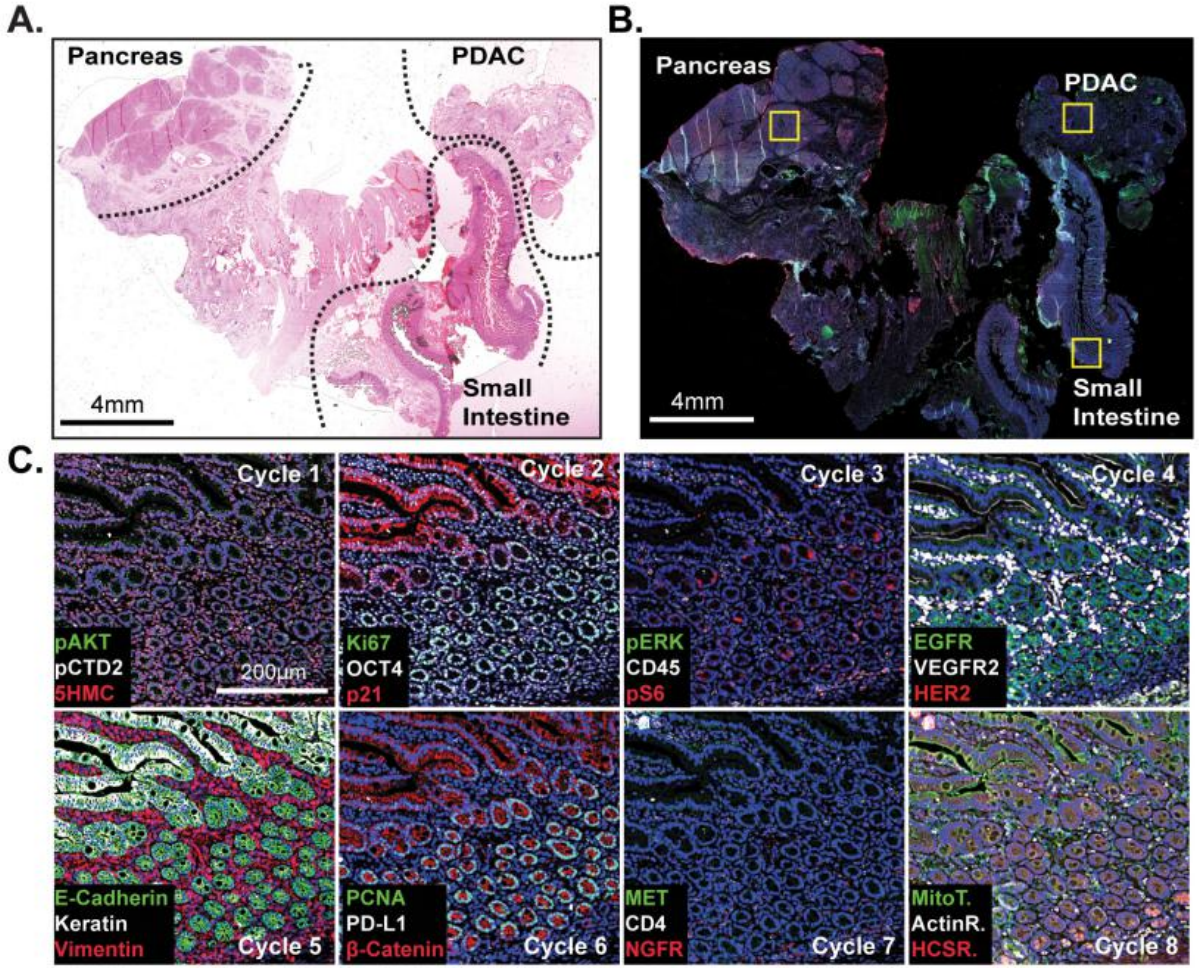

Differences in subcellular distribution were evident for many proteins, but for simplicity, they only analyzed fluorescence intensity on a per-antigen basis integrated over each whole cell.

plotting intensity value onto the segmentation data

computing correlations on a cell-by-cell basis

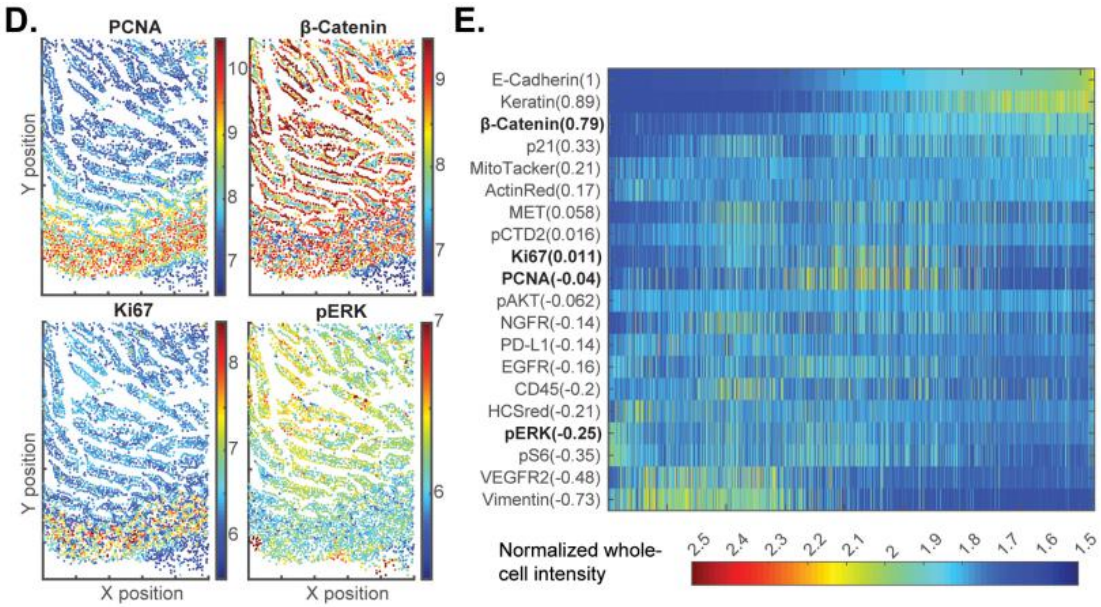

D) Segmentation data for four antibodies;
the color indicates fluorescence intensity (blue = low, red = high).

E) Quantitative single-cell signal intensities of 24 proteins (rows) measured in ~4X10 3 cells (columns) from panel (C)

Analysis of large specimens by t-CyCIF

High-dimensional single-cell analysis of human pancreatic cancer sample with t-CyCIF.

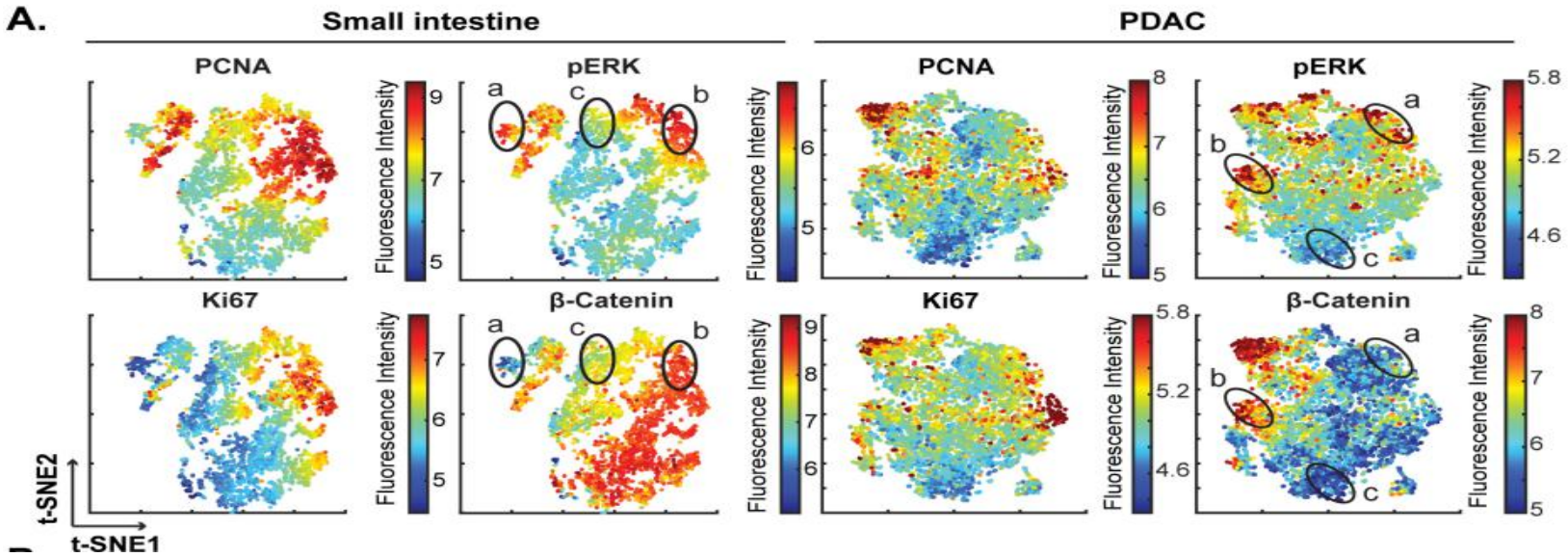

stochastic neighbor embedding (t-SNE) clusters cells in 2D based on their proximity

t-SNE plots of cells derived from small intestine or the PDAC region:
fluorescence intensities for markers of proliferation (PCNA and Ki67) and signaling (pERK and b-catenin) overlaid on the plots as heat maps.

--> In both tissue types, there exists substantial heterogeneity: circled areas indicate the relationship between pERK and b-catenin levels in cells and represent:
negative (‘a’),
positive (‘b’)
no association (‘c’)
between these markers.

Analysis of large specimens by t-CyCIF

High-dimensional single-cell analysis of human pancreatic cancer sample with t-CyCIF.

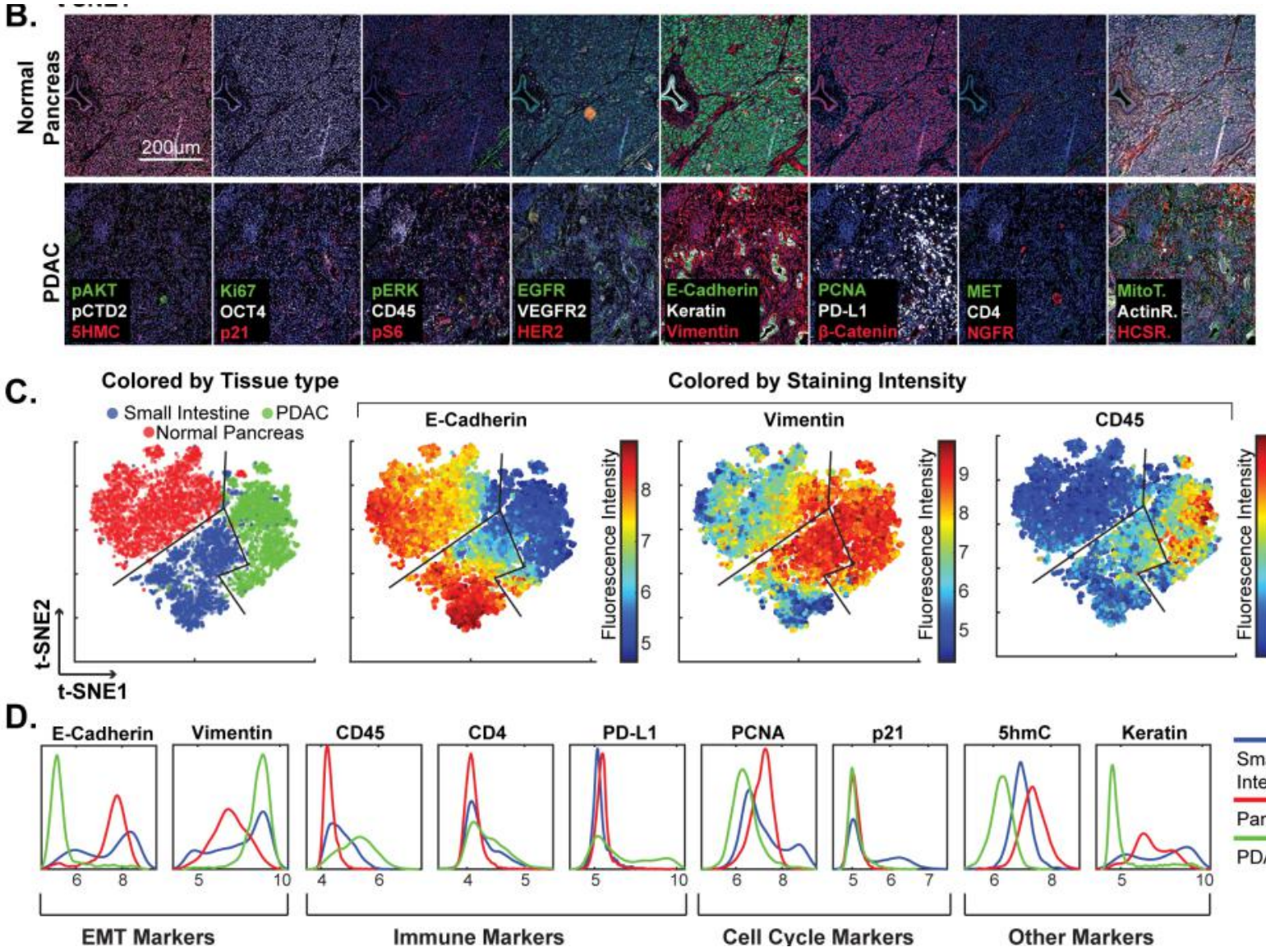

Vimentin and E-Cadherin had very different levels of expression in PDAC and normal pancreas as a consequence of:

- epithelial-to-mesenchymal transitions (EMT) in malignant tissues

- the presence of a dense tumor stroma, a desmoplastic reaction that is a hallmark of the PDAC microenvironment

Analysis of large specimens by t-CyCIF_observations

The capacity to image samples that are several square centimeters in area with t-CyCIF can facilitate the detection of signaling biomarker heterogeneity.

Gating for Ki67 high and PCNA high --> malignant --> again evidence of different relationships between pERK and b-catenin levels on a cellular level.

- Full range of possible relationships between the MAPK and WNT signaling pathways described in the literature can be found within a specimen from a single patient.

- Impact of tissue context on the activities of key signal transduction pathways.

Multiplex imaging of immune infiltration

Tumor immuno-profiling will yield biomarkers predictive of therapeutic response in individual patients.

- Responses of immuno-oncology drugs are variable across and within cancer types.
- The hope is that tumor immuno-profiling will yield biomarkers predictive of therapeutic response in individual patients.
- By measuring PD-1, PD-L1, CD4 and CD8 by IHC on sequential tumor slices, it was possible to identify some immune checkpoint inhibitor-responsive melanoma patients.

To test t-CyCIF in this application:

--> eight-cycle imaging was performed on a 1X2 cm specimen of clear-cell renal cell carcinoma using:
10 antibodies against multiple immune markers
12 against other proteins expressed in tumor and stromal cells

Multiplex imaging of immune infiltration

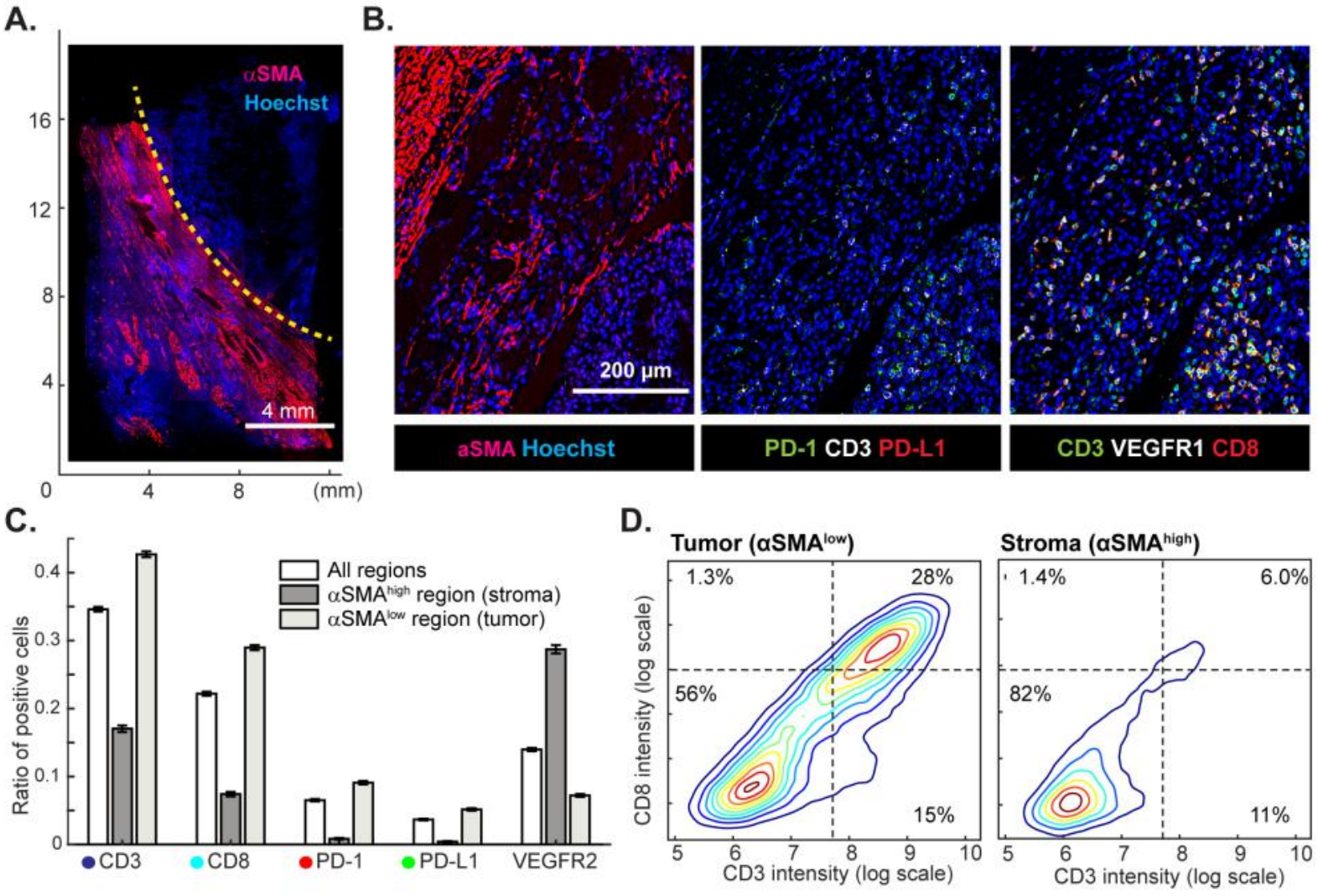

--> alpha-SMA high : regions denote stroma
--> alpha-SMA low : regions high density of malignant cells.

- In the a-SMA low domain, CD3 + or CD8 + lymphocytes were fourfold enriched
- PD-1 and PD-L1-positive cells were 13 to 20-fold more prevalent as compared to the surrounding tumor stroma
- CD3 + CD8 + double positive T-cells were found almost exclusively in the tumor.

↓

Suppression of immune cells is mediated by binding of PD-L1 ligand, which is commonly expressed by tumor cells, to the PD1 receptor expressed on immune cell.

Multiplex imaging of immune infiltration

Quantification of the degree of colocalization of cells expressing PD-1 + and PD-L1

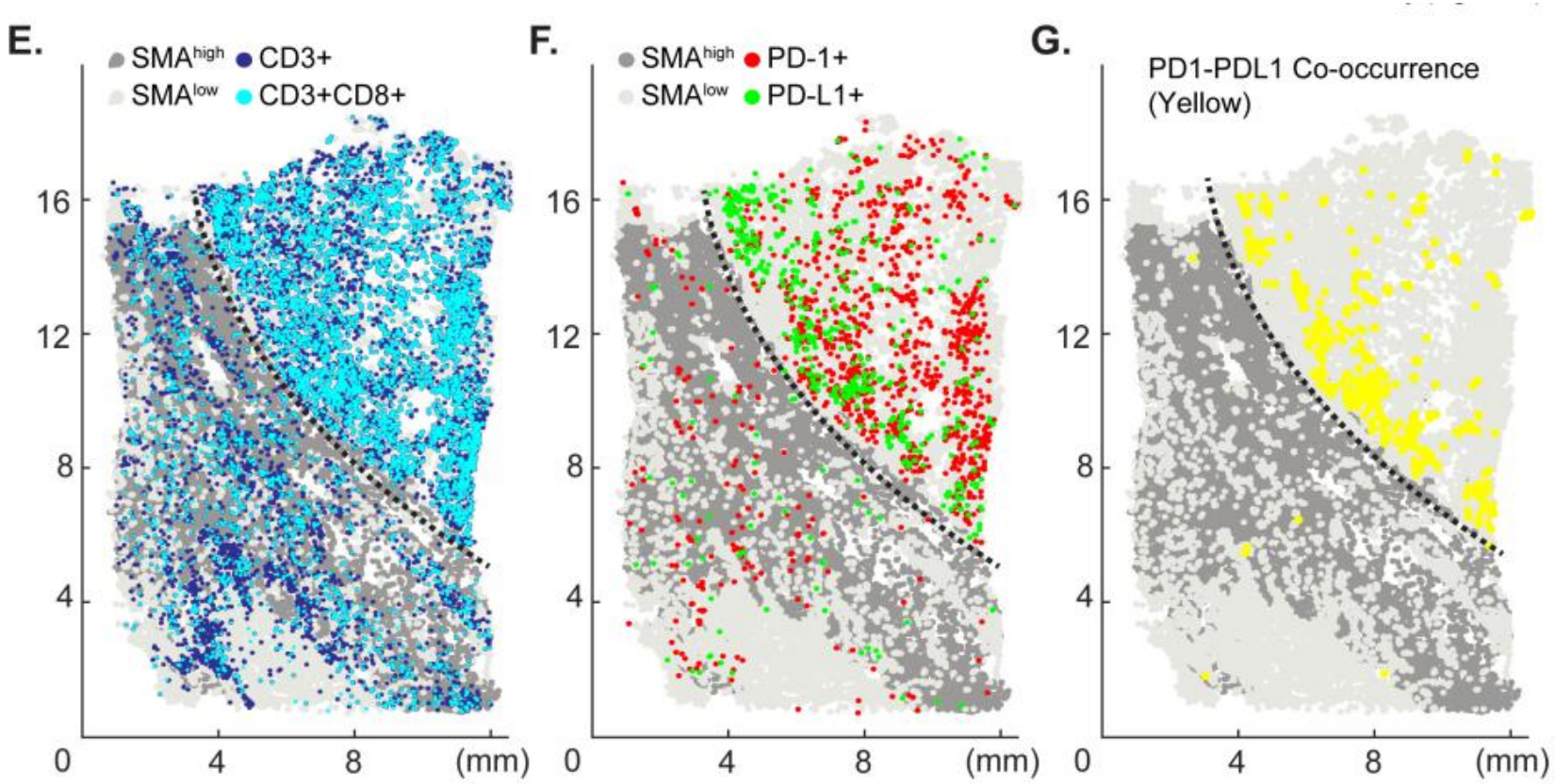

Demostration of:
-> Potential of spatially resolved immuno-phenotyping to quantify state and location of tumor infiltrating lymphocytes;
-> Prediction of biomarkers sensitivity to immune checkpoint inhibitor.

Analysis of diverse tumor types and grades using t-CyCIF of tissue microarrays (TMA)

-> Eight cycle t-CyCIF to TMAs containing 39 different biopsies from 13 healthy tissues and 26 biopsies corresponding to low- and high-grade cancers from the same tissue types
-> t-SNE and clustering on single-cell intensity data

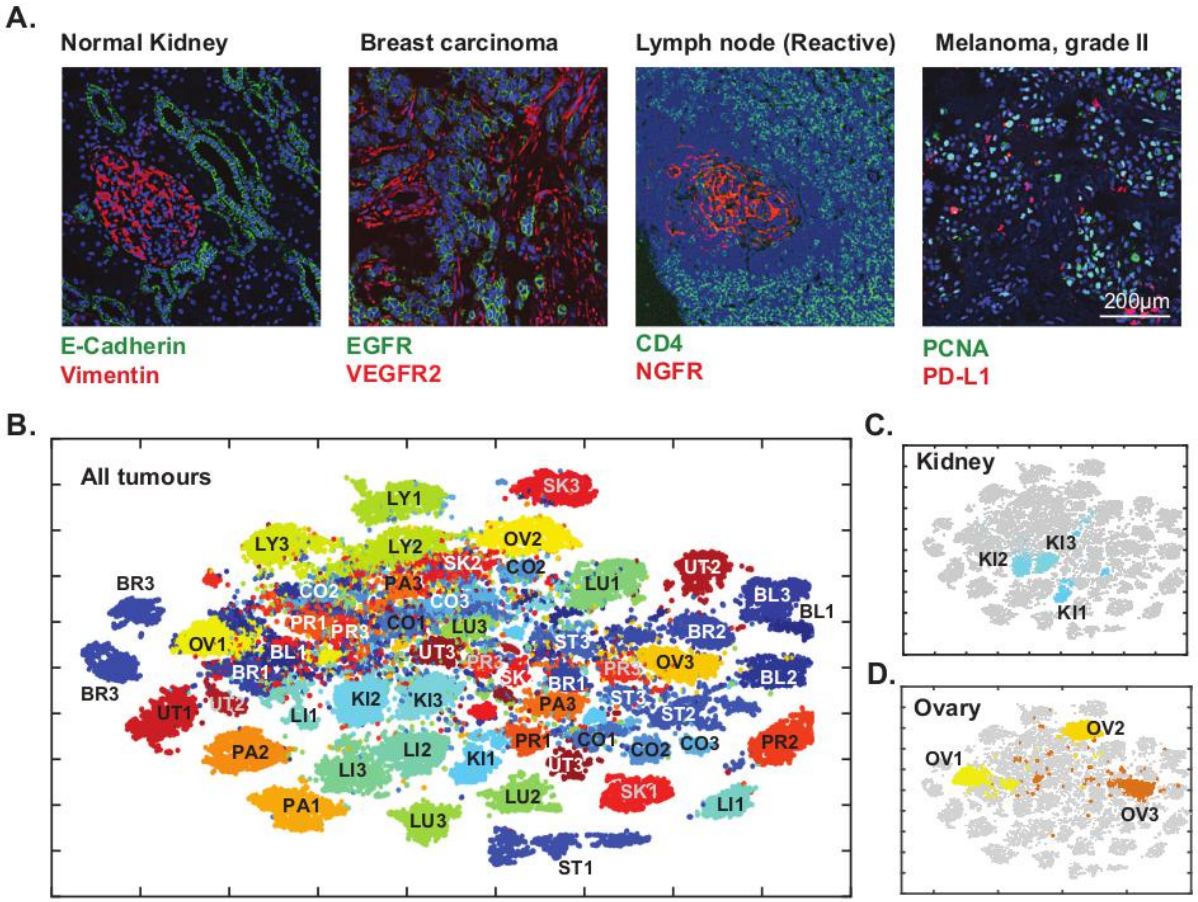

C) The great majority of TMA samples mapped to one or a few discrete locations in the t-SNE projection (e.g.: compare normal kidney tissue - KI1, low-grade tumors - KI2, and high-grade tumors – KI3.
D) Ovarian cancers were scattered across the t-SNE projection

In a number of cases, high-grade cancers from multiple different tissues of origin co-clustered, implying that transformed morphologies and cell states were closely related.

Analysis of diverse tumor types and grades using t-CyCIF of tissue microarrays (TMA)

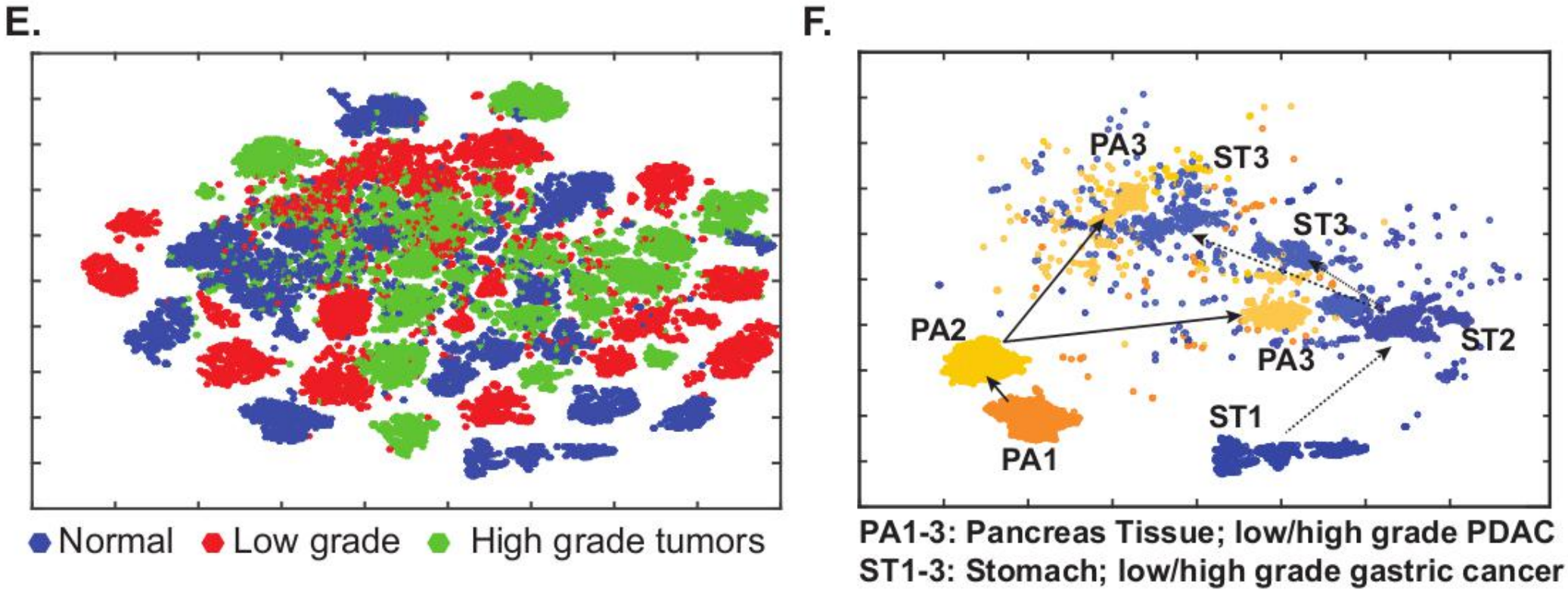

no separation between normal tissue and tumors regardless of grade

high-grade cancers from multiple different tissues of origin co-clustered
--> implying that transformed morphologies and cell states were closely related.

BUT: While healthy and low-grade pancreatic and stomach cancer occupied distinct t-SNE domains, high-grade pancreatic and stomach cancers were intermingled and could not be readily distinguished

Quantitative analysis reveals global and regional heterogeneity and multiple histologic subtypes within the same tumor in glioblastoma multiforme (GBM)

- Data from single-cell genomics reveals extensive heterogeneity in many types of cancer
- This phenomenon requires spatially resolved data

Eight-cycle imaging on a 2.5 cm x 1.8 mm resected glioblastoma (GBM) specimen imaging markers of neural development, cell cycle state and signal transduction

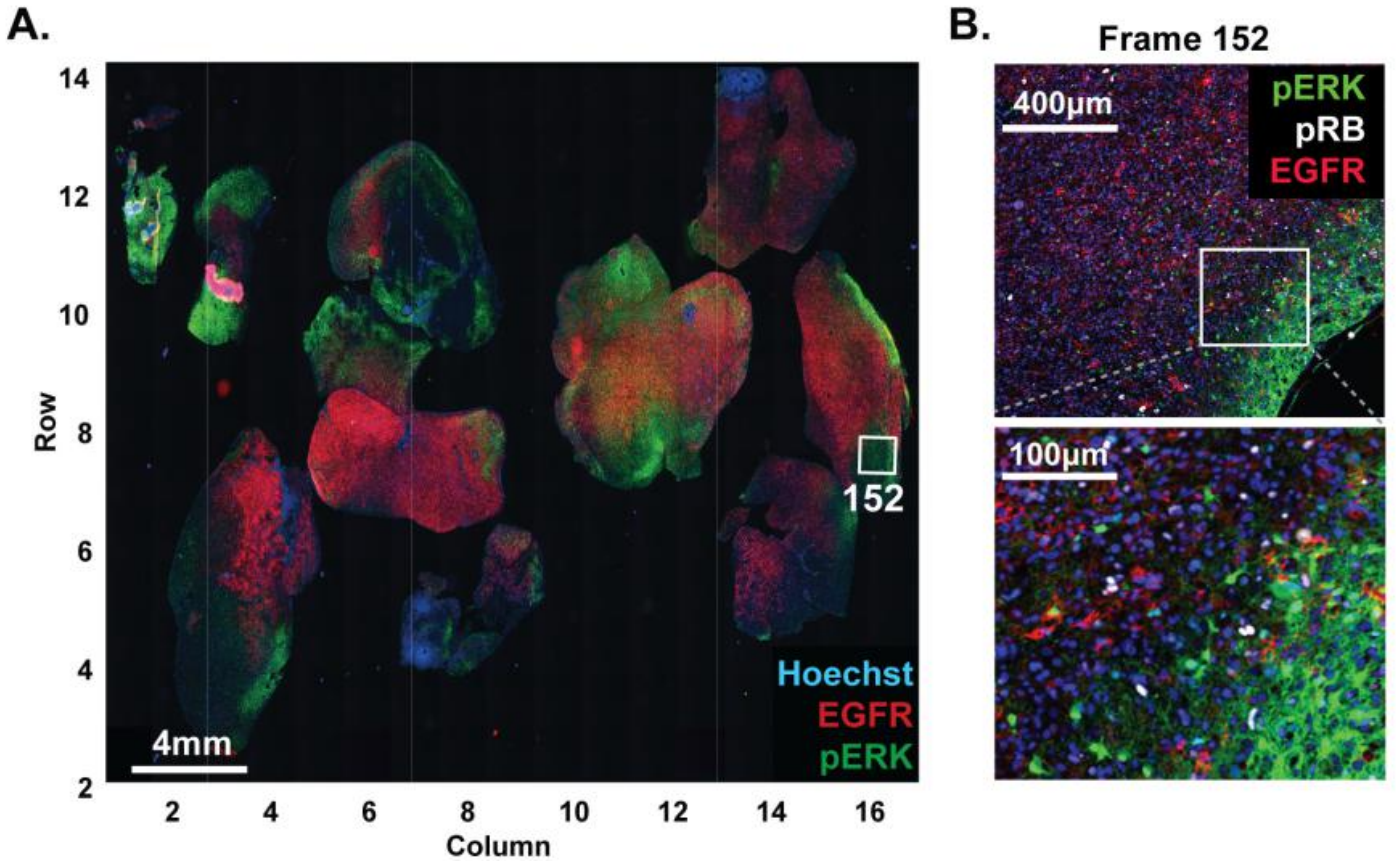

EGFR: Epidermal growth factor receptor

pRB: tumoral suppressor.

PERK: protein kinase RNA-like endoplasmic reticulum kinase

Quantitative analysis reveals global and regional heterogeneity and multiple histologic subtypes within the same tumor in glioblastoma multiforme (GBM)

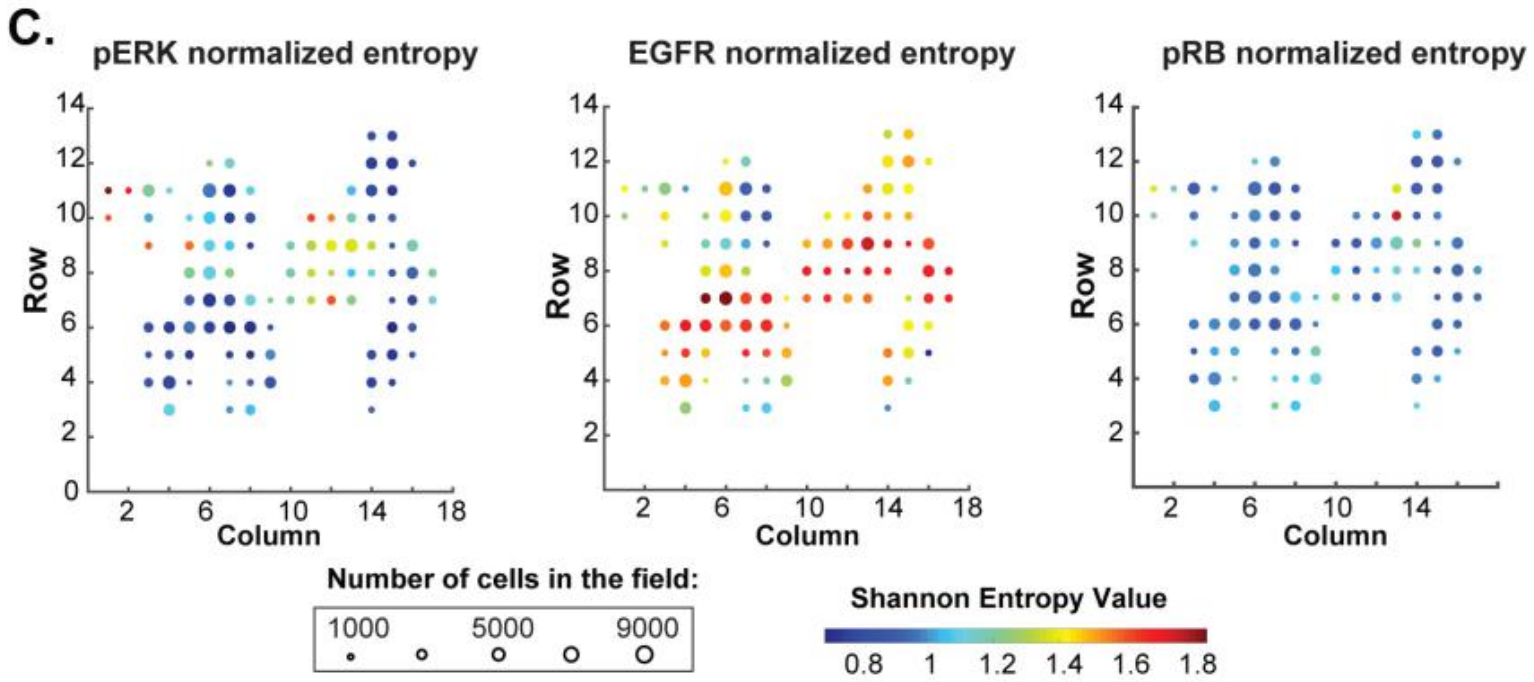

The extent of local heterogeneity varied with the region of the tumor and the marker being assayed.

To quantify local heterogeneity:
computed the informational entropy on a-per-channel basis for 1000 randomly selected cells in each field.

-> For a marker such as EGFR, which can function as a driving oncogene in GBM, informational entropy was high in some areas (red dots) and low in others (blue dots).

Quantitative analysis reveals global and regional heterogeneity and multiple histologic subtypes within the same tumor in glioblastoma multiforme (GBM)

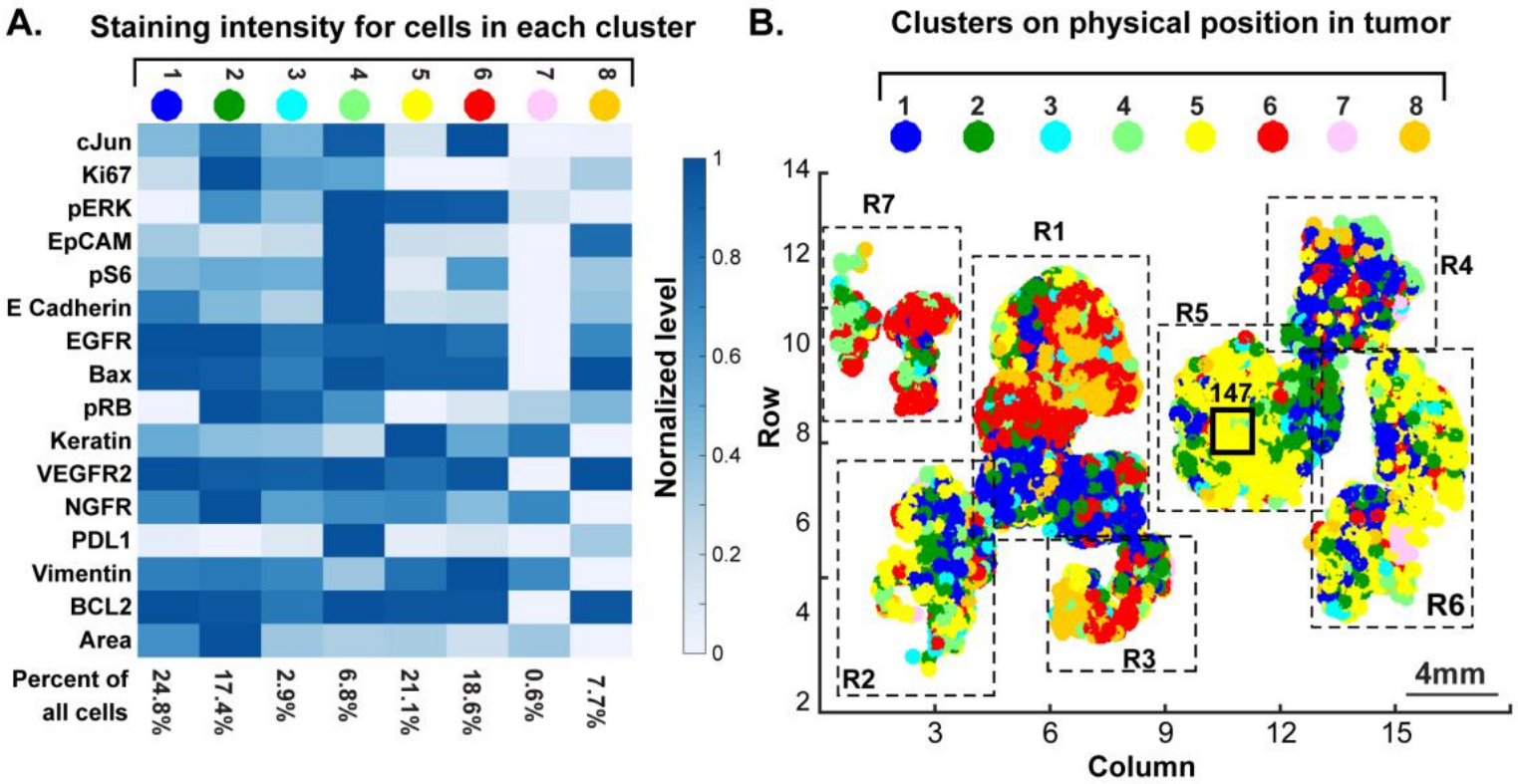

cluster one: high EGFR levels,
cluster two: high NGFR and Ki67 levels
cluster six: had high levels of vimentin
cluster five:high keratin and pERK levels

↓

The presence of four highly populated t-CyCIF clusters is consistent with data from single-cell RNA-sequencing of ~400 cells from five GBMs (Patel et al., 2014).

Quantitative analysis reveals global and regional heterogeneity and multiple histologic subtypes within the same tumor in glioblastoma multiforme (GBM)

To study the relationship between phenotypic diversity and tumor architecture

mapped each cell to an expectation–maximization Gaussian mixture (EMGM) cluster --> spatial probability distributions.

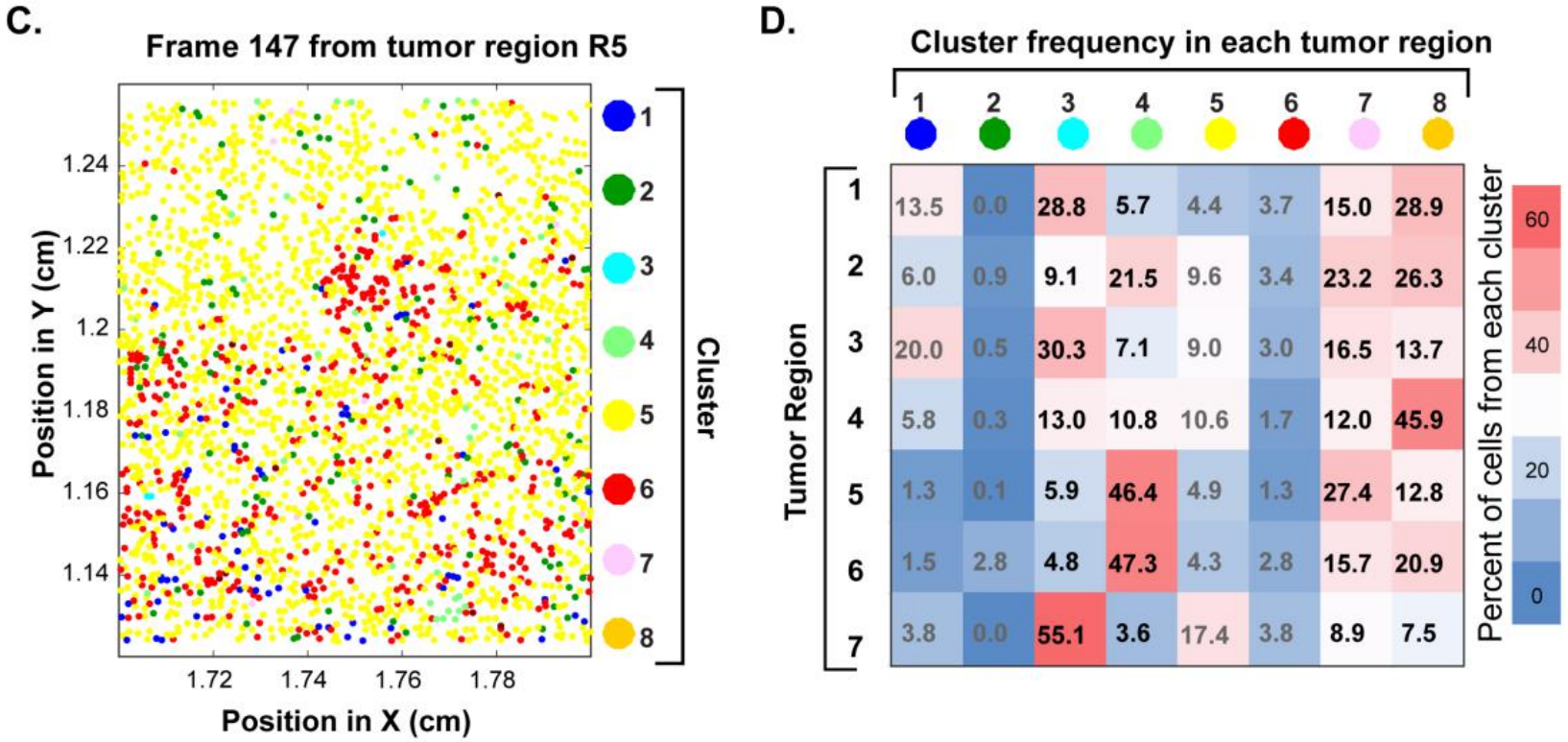

- GBM is phenotypically heterogeneous on a spatial scale of 5–1000 cell diameters.
- Cells corresponding to distinct t-CyCIF clusters are often found in the vicinity of each other.
- Sampling a small region of a large tumor has the potential to misrepresent the proportion and distribution of tumor subtypes.

Outlook_paper #2

- **t-CyCIF implementation of cyclic immunofluorescence is compatible with a wide range of antibodies** and tissue types and yields up to 60-plex images with excellent preservation of small intracellular structures.
- Multiscale imaging makes it possible to **combine tissue-level architecture with subcellular morphology**, much like a pathologist switching between low- and high-power fields, but there is little chance that such capabilities can be combined in a single instrument.
- t-CyCIF can use highly optimized filter sets and fluorophores, resulting in **good sensitivity.**
- t-CyCIF antibody panels are also simple to assemble and validate using **commercial antibodies,** including those that constitute FDA-approved diagnostics.
- **t-CyCIF is compatible with H&E staining,** enabling fluorescence imaging to be combined with conventional histopathology review.
- t-CyCIF method described here can **easily be implemented in a conventional research or clinical laboratory** without the need for expensive equipment or specialized reagents.
- t-CyCIF is relatively slow when performed on a single sample, but when many large specimens or TMAs are processed in parallel, throughput is limited primarily by imaging acquisition, which is at least as fast as approaches involving laser ablation.
- When samples are stained with the same antibodies in different t-CyCIF cycles, **repeatability is high** (as measured by correlation in staining intensity on a cell-by-cell basis) as is reproducibility across two successive slices of tissue (as measured by overlap in intensity distributions).
- The full range of discordant observations found in the literature can be recapitulated within a single tumor, emphasizing the wide diversity of signaling states observable at a single-cell level.
- Although it is not yet possible to link t-CyCIF clusters and known histological subtypes, **cell-to-cell heterogeneity on these spatial scales are likely to impact the interpretation of small biopsies.**

Conclusions_paper #2

- **t-CyCIF** is a robust, easy to implement approach to **multi-parametric tissue imaging applicable to many types of tumors** and tissues.
- It allows investigators to mix and match antibodies depending on the requirements of a specific type of sample.
- http//www.cycif.org ->antibody lists, protocols and example data.
- The resulting ability to quantify cell-to-cell heterogeneity may enable reconstruction of signaling network topologies in situ, by exploiting the fact that protein abundance and states of activity fluctuate from one cell to the next.
- When fluctuations are well correlated, they are likely to reflect causal associations.

Next important task:

cross-referencing tumor cell types identified by single-cell genomics or multi-color flow cytometry with those identified by multiplexed imaging
->possibility to precisely define the genetic geography of human cancer and infiltrating immune cells.

Thank you for your attention!